metals

MDPI

Review

Progress on Electrodeposition of Metals and Alloys Using Ionic Liquids as Electrolytes

Javan Grisente dos Reis da Costa, Josiel Martins Costa * and Ambrósio Florêncio de Almeida Neto

Laboratory of Electrochemical Processes and Anticorrosion, Department of Product and Process Design, School of Chemical Engineering, University of Campinas, Avenida Albert Einstein, 500, Campinas 13083-852, SP, Brazil
* Correspondence: josiel.martins.costa@gmail.com

Abstract: The electrodeposition process of metals and their alloys is widely used in the automotive, space, electronics, computing, jewelry, and other consumer items industries. Over the years, the search for new coatings with more suitable characteristics for their application led to the use of ionic liquids (ILs) as electrolytic solutions. In addition to having good conductive properties, the growing interest in these solvents has environmental appeal due to their low toxicity. Furthermore, the ability of these electrolytes to dissolve compounds containing less soluble metals makes them potential substitutes for environmentally harmful solvents. In this sense, this review describes the current state and the innovations concerning the electrodeposition of metals and alloys using ILs as electrolytes in the last five years. Metals were classified into five groups (common, light, noble, rare earth, and others), highlighting not only the ability to form a smooth, homogeneous, and anti-corrosive deposit, but also the reactive capacity of metals in hydrogen evolution and catalytic processes.

Keywords: batteries; coating; corrosion; electroplating; electrochemistry

Citation: Costa, J.G.d.R.d.; Costa, J.M.; Almeida Neto, A.F.d. Progress on Electrodeposition of Metals and Alloys Using Ionic Liquids as Electrolytes. *Metals* **2022**, *12*, 2095. https://doi.org/10.3390/met12122095

Academic Editor: David M. Bastidas

Received: 14 November 2022
Accepted: 2 December 2022
Published: 6 December 2022

1. Introduction

Among the main coating processes, electrodeposition stands out as a fast, low-cost method, in which the thickness of the deposit is easy to control. It is widely used in the automotive, aerospace, and oil industries [1]. In addition, electrodeposition has applications in the metallurgy and jewelry industries. This process is based on the mass transport of the solvated ion from the interior of the electrolyte solution toward the cathode. Adsorption of the coating metal occurs due to its complete desolvation and total charge loss (electron transfer) at a convenient location on the cathode surface. The atoms clump together until they form a growth center. This step is known as nucleation, and subsequent crystal growth occurs, controlled by interfacial phenomena. The interaction between these growth nuclei occurs through the superposition of crystals, giving rise to the growth of multilayers on the electrolytic surface, as shown in Figure 1 [2]. Although the process is known, the requirement to meet performance criteria has required ways to improve the electrolytic bath. Depending on application and service conditions, criteria include adhesion, ductility, and corrosion resistance [3,4].

Electrodeposition is categorized into the following three processes: (1) Underpotential deposition, (2) Electrophoretic deposition, and (3) Electroplating. Its main advantages and disadvantages are shown in Figure 2. Underpotential deposition is used in one- and two-step bimetallic particle syntheses. The metal is reduced on a surface at a potential less negative than the Nernst potential for the reduction of the metal on itself. Therefore, the reduction of the host metal is more favorable, forming monolayers or submonolayers of the secondary metal. On the other hand, electrophoretic electrodeposition generally uses two-electrode cells. The direct current electric field causes the charged particles to move towards the oppositely charged electrode, forming a compact and homogeneous film. Finally, electroplating employs an electric current to reduce dissolved metal cations in solution, forming a thin coating on the surface of the electrode.

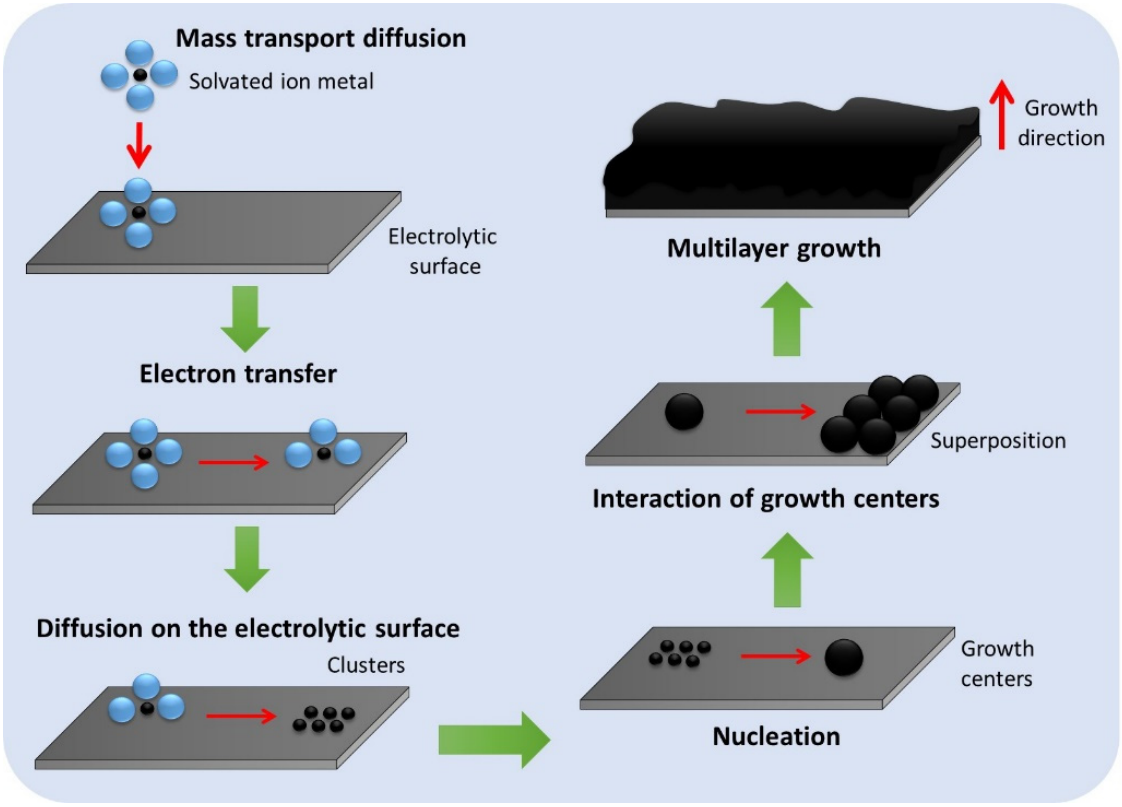

Figure 1. Deposit formation process and its involved phenomena.

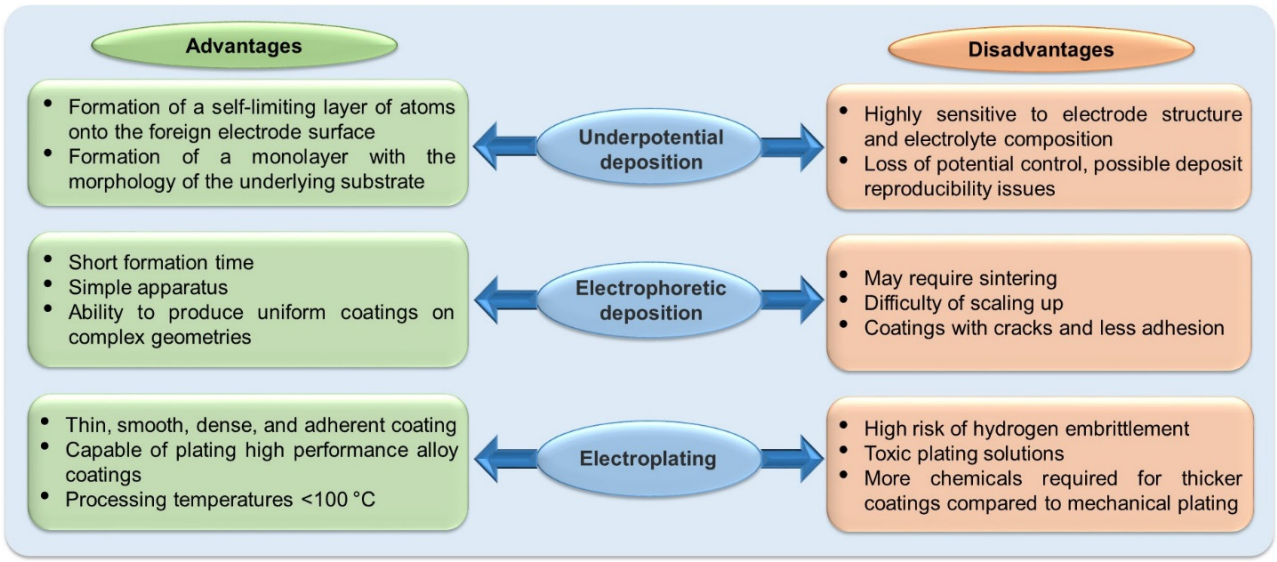

Figure 2. Main advantages and disadvantages of electrodeposition processes.

Al and its alloys are widely synthesized by electrodeposition. The studies use different aqueous baths, such as molten inorganic salts, organic solvents, and ionic liquids (ILs) [5]. ILs emerged as "green solvents" due to their easy incorporation into systems that were previously mostly dominated by volatile organic solvents. These salts are non-flammable, have a low melting temperature (<100 °C), have good thermal stability, and an almost insignificant vapor pressure [3,6]. In addition to being ecologically friendly, due to their low toxicity, they are easily recovered by extraction or distillation and recycled for subsequent use [7–9]. The composition of ILs (generally organic salts) comprises large cations derived from N-alkyl ammonium, phosphonium, sulfonium, guanidinium, imidazolium, pyrazolium,

pyridinium, and others, and are linked to anions with a delocalized or shielded charge such as bis(triflyl)imide, hexafluorophosphate, tetrafluoroborate, trifluoromethylsulfonate, dicyanamide, bromide, chloride, tetrachloroferrate(III), and others [3].

One of the main features of ILs is the flexibility to adjust and adapt their thermophysical properties by varying the constituent ions [6,7]. This flexibility reflects the ability to chemically and structurally modify the ionic pairs, resulting in various forms of application such as solvents, electrolytes, solar cells, gas storage, organometallic and enzymatic catalysis, lubricants, hydraulic fluids, and others, making it a valuable product for many kinds of research [3].

As displayed in Figure 3, the increase in the number of studies related to electrodeposition using ILs has been growing over the years. They have a wide electrochemical window and good electrical conductivity. The higher speed of the process, with very negative redox potential and no hydrogen evolution, can result in a low risk of corrosion to the equipment, including increased mass transfer and better control of the nucleation process and growth of deposit grains [10]. Another important factor is that they can be aprotic, which can solve questions concerning hydrogen ions in protic solvents [6].

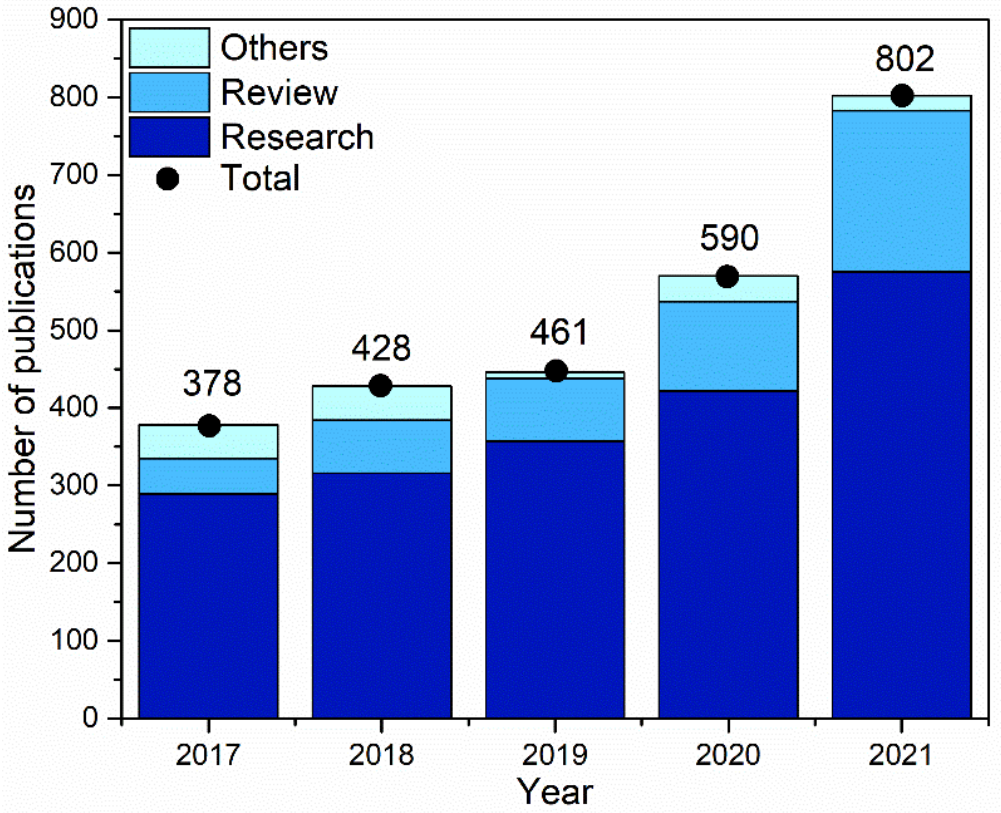

Figure 3. Number of articles per year containing the word 'electroplating ionic liquid solution' in the titles, keywords, and abstract section.

Table 1 summarizes the review for ILs for the electrodeposition of metals and metal alloys, and presents the organic salts, metals and alloys deposited. A combination of 79 ILs, 25 metals, and 40 alloys were found. Low-viscosity ILs are preferred in metal and alloy electrodeposition studies due to their ease of synthesis and stability under oxidative and reducing conditions [6,11]. However, some ILs have a high viscosity and can be a diminutive factor for mass transfer, making the process slower than aqueous electrolytes [10]. Therefore, they can also be presented from a mixture of deep eutectic solvents (DES). For example, choline chloride has a viscosity of 14.2 mm^2/s. In some studies, proportions are made with urea and/or ethylene glycol [12–15] to reduce the viscosity and obtain a lower melting point than pure components, improving mass transfer [16–18].

Table 1. Studies involving electrodeposition of metals and alloys with ILs in the last five years.

Nomenclature	Abbreviation	Metal or Alloy	Reference
(1-methyl-3-(2-oxo-2-((2,4,5 trifluorophenyl)amino)ethyle)-1H-imidazol-3-ium iodide)	[MOFIM]I	Ni–Co	[19,20]
1-(4-fluorobenzyl)-3-(4-phenoxybutyl)imidazole-3-ium bromide	[FPIM]Br	Co	[19,21]
		Ni	
		Ni–Co	[20]
1,3-dibutylpyrazolium bromide	DBPz–Br	Ag	[22]
1,3-dibutylmorpholinium bromide	DBMp–Br	Ag	[22]
1,3-dimethyl-2-imidazolidinone–$AlCl_3$	DMI−$AlCl_3$	Al–Mg	[23]
1,3-dimethyl-2-imidazolidinone–$LiNO_3$	DMI–$LiNO_3$	La	[24]
		Nd	[25,26]
1,3-dimethyl-2-imidazolinone–$ZnCl_2$	DMI−$ZnCl_2$	Zn	[27]
		Nd	[26]
1-alkyl-3-methylimidazolium bromide	EMIBr	Au	[28]
		Ag	[29]
1-allyl-3-methylimidazolium bromide	AMIBr	Zn	[30]
		Pt	[31]
1-butyl-1-methyl-pyrrolidinium bis(tri-fluoromethylsulfonyl) imide	[Bmim]TFSA or [BMPTFSA] or BMPyrrFSI	Cu	[32]
		Co	[33]
		Zn	[34]
		Al–Co	[35]
		Al–Cu	[35]
		Pr	[36]
		Bi	[36]
		Ti	[37]
		Ta	[38]
1-butyl-1-methylpyrrolidinium dicyanamide	[BMP][DCA]	Sm	[39]
		Ga	[40]
		Au	[41]
		Eu	[42]
		Cr	[43]
		Ag	[41,44,45]
1-butyl-1-methylpyrrolidinium triflate	BMPyOTf	Dy	[46]
1-butyl-1-methylpyrrolidinium trifluoromethylsulfonate	[BMIM][OTf] or [$Py_{1,4}$]TfO	Fe–Cu	[41]
		Fe–Al	[47]
1-butyl-3-(1-methylimidazolium-3-hexyl) imidazolium bromide		Ag	[29]
1-butyl-3-benzimidazolium bromate	[HBBIm]Br	Pd	[48]
		Pt	[48]
1-butyl-3-butyillimidazolium bromide	DBIz–Br	Ag	[22,29]

Table 1. *Cont.*

Nomenclature	Abbreviation	Metal or Alloy	Reference
1-butyl-3-methylimidazolium–hydrogen sulfate	[BMIM]HSO_4	Ni–Fe	[49]
1-butyl-3-methylimidazolium acetate	[Bmim][Ac]	Cd–Te	[50]
1-butyl-1-methylpyrrolidinium dicyanamide	[BMP][DCA]	Ag	[41,44]
		Eu	[42]
		Sm	[39]
		Cr	[43]
		Ga–Sb	[40]
1-butyl-1-methylpyrrolidinium triflate	BMPyNTf	Dy	[46,51]
1-butyl-3-methylpyrrolidinium dicyanamide	[BMIm][DCA]	Ag	[41]
1-butyl-3-methylimidazolium bis(triflyl)imide	[BMIM][TFI] or C_4mimTFSA	Ni–Fe	[52]
		Cu	[32]
1-butyl-3-methylimidazolium bromide	[Bmim][Br]	Ag	[29,53]
1-butyl-3-methylimidazolium chloride	[Bmim][Cl] or [BMIC] or [C_4mimCl]	Al	[54–61]
		Al–Ti	[62]
		Ti–Al	[63]
		Ag–Pd	[64]
		Cu–Sn	[65,66]
		Cu–Ag	[67]
		Pd	[68]
1-butyl-3-methylimidazolium hexafluorophosphate	[Bmim]PF_6	Ru	[69]
		Ir	[70,71]
1-butyl-3-methylimidazolium tetrafluoroborate	[BMIm][BF_4]	Co	[72]
		Ir	[73]
		Ce	[74]
1-butyl-3-methylimidazolium trifluoromethanesulfonate	[Bmim][TfO]	Zn	[75]
		Sn	
1-butyl-3-methylimidazolium dicyanamide	[BMIm][DCA]	Ag	[41]
		Au	[41]
		Cu–Sn	[76]
1-butylimidazolium bromide	[HBIm][B]	Ag	[53]
1-decyl-3-(1-methylimidazolium-3-hexyl) imidazolium bromide		Ag	[29]
1-dodecyl-3-methylimidazolium chloride	[C_{12}mim][Cl]	Ni–Fe–Mo	[77]
		Ni–Fe–W	
1-ethyl-3-methyl imidazolium bromide	[EMIM] [Br]	Ni–Mo	[78,79]

Table 1. *Cont.*

Nomenclature	Abbreviation	Metal or Alloy	Reference
1-ethyl-3-methylimidazolium chloride	[EMIM][Cl] or [EMIC] or [C_2mimCl]	Zn	[80]
		Nd–Fe	[81]
		Al	[11,54,82–90]
		Al–Li	[91]
		Al–Ga	[92]
		Al–Mn–Zr	[93]
		Al–Ti	[94]
		Al–W	[95–97]
		Al–Mn	[98]
		Co–Zn	[99]
		Cu	[100]
		Cu–Sn	[101]
		Ga	[102]
		Pd	[103,104]
1-ethyl-3-methylimidazolium chloride-ethylene glycol	EMIC–EG	Ni–La	[105]
1-ethyl-3-methylimidazolium chloride–urea	EMIC–UA	Cu	[100]
1-ethyl-3-methylimidazolium dicyanamide	[EMIM][DCA]	Cu–Sn	[76]
		Nd	[81,106]
		Fe	[81,106]
		Nd–Fe	[81]
1-ethyl-3-methylimidazolium trifluoroacetate	[Emim]TA	Pd	[107]
1-ethyl-3-methylimidazolium trifluoromethylsulfonate	[EMIm][TfO]	Cu–Zn	[108]
		Cu	[109]
		Ag	[109]
1-ethyl-3-methylimidazolium bis(trifluoromethylsulfonyl)imide	[C_4mim][NTf_2]	Ga	[102]
		Pd	[110]
1-ethyl-3-methylimidazolium bis(fluorosulfonyl)amide	[C_2C_1im][FSA]	Na	[111]
1-ethyl-3-methylimidazolium fluoride	[EMIM]F	Cu	[112]
1-heptyl-3-(1-methylimidazolium-3-hexyl) imidazolium bromide		Ag	[29]
1-hexyl-3-methyl-imidazolium bromide	[HMI][Br]	Ag	[29]
1-hexyl-3-methyl-imidazolium chloride	[HMI][Cl]	Al	[54]
1-ethyl-1-methylpyrrolidinium bis(trifluoromethylsulfonyl) imide	[EMIm][TFSA]	Cu	[113]
		Cu–Sn	[114]
		Zn	[34,115,116]
1-hexyl-3-methylimidazolium hydrogen sulfate	[HMIM][HSO_4]	Ag	[117]
1-Methylpiperidinium trifluoromethane sulphonate	[HmPip][OTf] or [MIMTfO]	Cu	[118]
		Zn	[119]
1-octyl-3-methylimidazolium bromide		Ag	[29]

Table 1. *Cont.*

Nomenclature	Abbreviation	Metal or Alloy	Reference
1-propyl-1-methylpyrrolidinium bis(trifluoromethanesulfonyl)amide	[C_3mpyr][TFSA]	Co	[120]
1-tetradecyl-2-aminoethyl imidazolium bromide	[C_{14}PImNH_2]Br	Pt	[121]
2,2-diheptyl-1,1,3,3-tetramethylguanidinium bromide		Pt	[122]
3- butyl-1- ethylimidazolium		Al	[61,123]
Aluminium chloride–4-ethylpyridine	$AlCl_3$–4-EP	Al	[124]
Aluminium chloride–triethylamine hydrochloride	$AlCl_3$–TMHC	Al–Zr–Cu	[125]
		Co–Al	[126]
Betainium bis((trifluoromethyl)sulfonyl)amide	[Hbet][Tf_2N] or [Hbet][TFSA]	Cu	[127]
		Cu–Pb	[127,128]
		Zn	[129]
		Pb	[129,130]
		Pd	[131]
Butylpyridinium dicyanamide	$Pyri_4$–DCA	Ag	[45]
Choline chloride–ethylene glycol	ChCl–EG	Fe–Cr	[132]
		Ni–Fe	[133]
		Ni–Sn	[134]
		Ni	[12,18,135,136]
		Ni–Sn–P	[137]
		Co	[138,139]
		Ni–Co	[15]
		Cu	[118,136,140]
		Sn	[136]
		Zn	[17,141–143]
		Au	[144]
		Ag	[136,144]
		Mn	[14]
Choline chloride–Urea	ChCl–UA	Ni	[12,18,145]
		Co	[139]
		Ni–Co	[13]
		Zn	[17]
		Mn	[14]
		Pr–Mg–Co	[146]
		Pr–Mg–Ni	[147]
		Sn–Co–Ni	[148]
		Sn–Co–Zn	
Choline chloride–malonic acid	ChCl–MA	Co	[139]
		Co–Cr	[149]
Choline chloride–oxalic acid	ChCl–OC	Co	[139]
Dibutylpyrrolidinium bromide	DBP1–Br	Ag	[22]

Table 1. *Cont.*

Nomenclature	Abbreviation	Metal or Alloy	Reference
Ethylene carbonate–Aluminum chloride	EC–$AlCl_3$	Al–Li	[150]
		Li	[150]
Lithium–bis(trifluoromethylsulfonyl)amide	Li–TFSI	Li	[151–153]
Lithium–bis(fluorosulfonyl)imide	Li–FSI	Li	[153]
Perfluoro-3-oxa-4,5 dichloro-pentan-sulphonate		Al	[154]
poly(1-allyl-3-methylimidazolium)	PAMI	Pt	[31]
Tetramethyl guanidinium-perfluoro-3-oxa-4,5 dichloro-pentan-sulphonate	$[C_5H_{14}N_3{}^+][CF_2ClCFClOCF_2CF_2SO_3{}^-]$	Al	[154,155]
Tributylhexylphosphonium bis(trifluoromethyl sulfonyl)imide	[P4446][NTf_2]	Li	[156]
Triethylammonium acetate	[TEAA]	Ag–Cu	[157]
Triethyl-n-pentyl phosphonium bis(trifluoromethyl-sulfonyl)amide	[P_{2225}][TFSA]	Ru	[158]
Triethyl-n-hexyl phosphonium bis(trifluoromethyl-sulfonyl)amide	[P_{2226}][TFSA]	Pt	[159]
Trihexyltetradecylphosphonium bis(2,4,4-trimethylpentyl)phosphinate	(Cyphos IL 104®)	Rh	[160]
Trihexyltetradecylphosphonium bis(trifluoromethylsulfonyl)amide	[$P_{6,6,6,14}$][TFSI]	Nd	[161]
Trihexyl(tetradecyl)phosphonium chloride	(Cyphos IL 101)	Ir	[162]
N-butyl-N-methylpyrrolidinium bistriflimide	BMPTFSI	La	[163]
		Sm	
		Nd	
		Dy	
N-butyl-N-methyl pyrrolidinium dicyanamide	BMP–DCA or [C_4mpyr][DCA]	Ni–La	[164]
		Nd	[165]
N-methyl-N-butyl-pyrrolidinium bis(trifluoromethanesulfonyl)imide	[C_4mpyr][Tf_2N]	Li	[166]
N-methyl-N-propylpiperidinium bis(trifluoromethanesulfonyl)imide	[MPPip][TFSI]	Zn	[167]

Among the metals, Al [5,85], Co [168], Ni [145], and Zn [169] appear more frequently in electrodeposition using ILs, mainly due to their protection characteristics and rapid mass transfer during the process. In addition, they are favorites to serve as base metals, including for alloys such as Fe [170] and Cu [108], since they perform efficient codeposition and rapid nucleation. Another strong application for ILs is the ability to dissolve salts or oxides of rare earth and noble metals and then perform their electrodeposition. The process separates the metal of interest from a complex mixture, making the application of ILs fundamental.

The oxidizing capacity of light metals (Na, Li, and Mg) can be better controlled using ILs in catalytic reactions in batteries, which can promote electroadsorption under less unstable conditions [111]. Therefore, these studies highlight the ability of ILs to replace organic solvents. In this context, the review proposed a valuation and critical analysis of the use of ionic liquids in the electrodeposition process of metals and alloys in the last five years.

2. Electrodeposition of Common Metals

2.1. Aluminum

Aluminum plays an essential role as an excellent coating material due to its thermal properties, electrical conductivity, light weight, and corrosion resistance [5]. In addition, Al coatings and alloys tend to develop a natural passive oxide layer on their surface during contact with air, making them resistant to corrosion in different environments [55]. In recent years, the electrodeposition of Al from ILs has generated great interest among academic and industry researchers due to its industrial potential, benefiting many industries such as automotive, aeronautics, naval, construction, electronics, and others [56]. The outstanding characteristics are the ability to operate at low deposition temperatures, ease of preparation, low cost, and high electrochemical stability. Furthermore, chloroaluminate ILs are the simplest compounds, containing inorganic halide anions and organic cations [171], which, in solution, form the ions $[(Al_2Cl_7)]^-$ and $[(AlCl_4)]^-$ as electroactive species available for reduction.

Several authors change the $AlCl_3$/IL molar ratio with the ionic cation to improve conductivity and electrochemical potential window and favor electroplating on an industrial scale. The feasibility of the electrodeposition process depends on the $AlCl_3$/IL molar ratio and the characteristic of the studied IL. For $[C_5H_{14}N_3{}^+][CF_2ClCFClOCF_2CF_2SO_3{}^-]$, the studied molar ratio ranged from 0.9 to 1.3. This composition range showed better conductivity values that allowed sufficient mobility of the electroactive species [155]. At room temperature, $[C_5H_{14}N_3{}^+][CF_2ClCFClOCF_2CF_2SO_3{}^-]$, due to its immiscibility in water, produced excellent deposits for an $AlCl_3$/IL molar ratio of 0.95:1 [154]. For $AlCl_3$/4-EP, the reduction current with a molar ratio of 1.3:1 was greater than that with a molar ratio of 1.1:1, suggesting that the reduction of $[AlCl_2(4\text{-}EP)_2]^+$ is thermodynamically favorable than $[AlCl_2(4\text{-}EP)_2]^+$ [124].

For BMIC, with a 1:2 molar ratio, the deposition of Al on a copper substrate was efficient at 90 °C [57]. In contrast, Wang et al. [58], inverting the proportion to 2:1, evaluated the temperature variation during the electrodeposition process of Al on Cu. They demonstrated that at 100 °C, there was a better diffusion and/or migration of $Al_2Cl_7{}^-$ ions, generating an increase in current density with a contribution to greater nucleation and efficiency of Al deposition. However, temperatures higher than room temperature may not favor electrodeposition on IL [59] since these conditions also depend on the IL and the porosity of the substrate [55].

The Al deposit studies have a rich variation of the $AlCl_3$/IL ratio. However, [EMIm]Cl stands out as the main IL for the electrodeposition of Al and its alloys [82,83]. The most evaluated $AlCl_3$/[EMIm]Cl ratio was 2:1 [11,84,85]. However, ratios between 1:1 and 2:1 [54,86] and 1:2 [83] also obtained excellent deposition results. [EMIm]Cl confers a less negative applied potential and a higher current density to Al deposition in addition to a uniform coating and instantaneous nucleation of the coating, promoting lower energy consumption during the deposition.

The lower energy consumption and uniform coating have sparked interest in the Li-ion battery field. For example, Peng et al. [87] studied [EMIm]Cl as an electrolyte for the deposition of Al on Ni. As a result, they obtained a film free of dendrites, improving the corrosion resistance of Ni, and making it suitable for use as anodes of Li-ion batteries. The smooth and uniform deposition was also obtained at a current density of 20 mA/cm^2 for the uranium substrate, significantly increasing the corrosion resistance [88]. Another recent advance was the magnetohydrodynamic (MHD) effect of the $AlCl_3$–[EMIm]Cl composition in reducing the activation energy required to promote electrochemical reduction [89]. In addition, it increased the capacitance of the electrical double layer and promoted greater mass transport of Al [90].

The $AlCl_3$/IL ratio inspires researchers to develop Al alloys from electrolytes containing ILs. Several alloys were synthesized in different temperature ranges, such as Al–Li [91] and Al–Ga [92] at 25 °C, Al–Mg [23] at 50 °C, and Al-Cu [35] at 70 °C. However, the two most cited Al alloys in the literature refer to Al–Ti and Al–W. The 2:1 $AlCl_3$–[EMIm]Cl elec-

trolyte containing TiCl4 (0.1 M) resulted in an Al–Ti alloy deposited on a copper electrode after a multi-step reduction [94]. The reduction to $TiCl_4^{2-}$ contributed to the codeposition of Ti on Al, with a Ti content of up to 7.37%. In contrast, Xu et al. [62], using [Bmim][Cl] as an electrolyte, obtained an Al–Ti alloy with a Ti content of up to 11.4 at.%.

Another study co-deposited Al on Ti (Ti–Al alloy) using [Bmim][Cl] [63]. The authors maintained the highest proportion of Ti of up to 40%, demonstrating that increasing the IL chain showed a greater ability to control the composition and morphology of Al–Ti coatings. For Al–W, as well as Al deposits, [EMIM][Cl] is the most used cation [95], with W contents in the range of 9–12 at.% using W_6Cl_{12} as the W source for AlC_3/EMImCl ratios 2:1 [96,97].

Unlike the studies cited, Higashino et al. [96] obtained a W content of 20 at.%, with a 1:1.5 ratio of $AlCl_3$/EMImCl, demonstrating that the increase in the cation made the electrolyte more polarizable. Furthermore, the increase in current density favored the codeposition of W over Al. Bright and adherent deposits of ternary alloys with Al have also been studied. However, the proportions of the other metals added together were at most 10%, demonstrating the need for a careful view of the proportions to favor the codeposition [93,125].

In addition, by evaluating parameters such as component proportions, temperature, and current density, additives have been highlighted in the electrolyte composition combined with IL for Al and its alloys. For [BMIM][Cl], additives such as dichloromethane (DCM) and toluene (C_7H_8) were evaluated as improving agents for Al electrodeposition processes [61]. The morphology of the deposits improved with DCM due to its interaction with the [BMIM][Cl] cations, which can be adsorbed on the protruding part of the electrode surface during the electrochemical process. On the other hand, as the interaction of C_7H_8 with the cation was low, the characteristics of the deposit were inferior to those of DCM.

For IL, 3-butyl-1-ethylimidazolium, light aromatic naphtha (LAN) [123], as well as DCM for [BMIM][Cl], also improved the morphology of the deposits due to attraction with the 3-butyl-1-ethylimidazolium cation, demonstrating a brighter appearance to the metal. Although the electrodeposition of Al and its alloys with the ILs in the electrolytic environment is already present in many studies, research on ternary alloys and additives that improve the electrodeposition process can be further explored.

2.2. Iron

Due to the ease of oxidation, Fe is one of the few metals not studied individually in electrodeposition processes. All studies used Fe as a base metal and inducer of the codeposition of other metals to obtain stable and anticorrosive alloys [132] or as an element codeposited by a base metal [133]. Fe–Cu [172] and Fe–Al [47] alloys were obtained by electrodeposition with $[Py_{1,4}]$TfO, both on a copper substrate, aimed to "damp" these alloys. For both studies, there was a thin deposition of the alloys on the substrate, in which the interaction phenomenon was charge transfer. The difference between the depositions was the locations of the damping peaks. For Fe–Cu, a damping peak occurred around 680 K, leading to the appearance of Fe particles at the interface between Cu and Fe (Cu + α-Fe phase). The driving force was the diffusion of Cu atoms around the Cu + α-Fe phase particles. For Fe–Al, the peak appeared around 800 K. However, the phenomenon depended on the dissolution of small precipitates or agglomerates of defects during heating. During cooling, the phenomenon depended on the reprecipitation/reagglomeration of the particles. Therefore, $[Py_{1,4}]$TfO favored the electrodeposition of Fe alloys, improving the damping of the process.

Although Fe is preferentially studied as an alloy, alloys with Ni were the most found considering Fe codeposited [49,77,133]. One of these studies aimed to improve the anticorrosion properties of the Watts bath of Ni–Fe alloy with boric acid [52]. $[BMIM]HSO_4$ improved the nucleation and three-dimensional growth of Ni–Fe alloy grains due to the increase in charge transfer involved in the process [49]. For the authors, the anticorrosive improvement was evident.

2.3. Nickel

Most studies involving Ni use the $NiCl_2$ salt as the metal source since the Cl ions, together with the ILs, show the viscosity and electrical conductivity of the medium can be improved, in addition to improving the Ni nucleation mechanism [12,145]. Baths containing choline chloride favor electrodeposition, generating instantaneous three-dimensional nucleation at negative potentials. In addition to urea, ethylene glycol can also form an IL with choline chloride for Ni deposition. Diffusion controls this process. In this way, the formation of nanostructured Ni films improves the surface area of the electrode, promoting an increase in the catalytic activity in the hydrogen evolution reaction [18].

Since Ni is an excellent inductor for the co-deposition of other metals, unusual metals have been co-deposited with Ni. Choline chloride with ethylene glycol was also crucial for depositing Ni–Sn [134] and Ni–Sn–P [137] alloys from ILs. Rosoiu et al. [134] deposited Ni–Sn by a pulsed and direct current. However, using pulsed current, the hardness of the Ni–Sn alloy showed better results. In another study, although the authors did not assess the hardness of Ni-Sn-P alloy synthesized from choline chloride-ethylene glycol, this alloy exhibited superior corrosion resistance to Ni-P coatings [137]. Furthermore, its corrosion resistance improved with increasing Sn content. According to Yang et al. [105], EMIC–EG (1:2 molar ratio) improved the induction of Ni to deposit Ni–La alloy with instantaneous nucleation and three-dimensional growth. In addition to the use of IL in the electrolyte solution, the control of current density and temperature resulted in the CFC or amorphous structure of the alloy.

The evaluation of catalytic activity during the electrodeposition of Ni and its alloys using ILs has been growing since ILs have significant effects on parameters such as current density, pH, and deposition time [135,173]. According to Gao et al. [164], the catalytic activity in BMP–DCA medium was verified due to low overpotentials (−279 mV) even operating at 100 mA cm^{-2}. This demonstrates that Ni–La or Ni–rare earth alloys can be important in the evaluation of hydrogen evolution processes. In addition to this process, Jesmani et al. [78] evaluated the electrocatalytic properties of Ni–Mo alloys for methanol oxidation in a modified Watts bath (EMIM [Br]). The increase in current density (from 1 to 6 A/dm^2) decreased the Mo content, reducing the catalytic activity of the process. The optimal current density was 3.5 A/dm^2, showing better catalytic performance. Likewise, another study with EMIM[Br] also showed excellent catalytic activity for the methanol oxidation process [79]. However, changes in pH directly interfered with current density. The best catalytic activity occurred at pH 7 with a current density of 15 mA/cm^2.

2.4. Cobalt

Cobalt and cobalt-based alloys are essential materials in many industrial and technological fields due to their magnetic properties, hardness, thermal stability, and corrosion resistance [138]. As a ferromagnetic, its applicability includes microelectronics, high-density magnetic storage media, spintronics, drug and gene delivery, and immunological magnetic separation [33,139]. However, most Co depositions show high overpotentials due to the formation of negatively charged metal complexes due to the coordination of anions at room temperature [120]. Therefore, studies seek external and internal modifications to improve the deposition of Co. Ries et al. [72], through a rigorous diffusional control, obtained a deposit of Co at 50 °C from a solution containing [BMI][BF_4], producing a diffusion coefficient of 8.21×10^{-10} cm^2 s^{-1}. In addition, the Co films were compact, smooth, shiny, and adherent to the substrate, resulting in crack-free metallic Co layers.

Alloys containing Co as the base metal has been little discussed recently in electrodeposition with ILs in the electrolyte solution composition [99,126,141]. However, as with Fe, studies report Co as a metal co-deposited by Ni since the ferromagnetic properties of these elements favor their affinity [13,15]. The peak reduction of the Ni–Co alloy can be observed between −0.6 and −1.2 V using choline chloride as the IL. The highest reduction peak occurred at −1.0 V, which favored the diffusional process deposited with 20 wt.% of Co [15]. However, by adding ethylene glycol to form a eutectic solvent, the diffusion

process reduced the Co content to about 12 wt.%. This reduction indicated a worsening in corrosion protection.

[MOFIM]I is considered to be a prominent additive for Watts baths of Ni–Mo alloys [20]. In contrast, [FPIM]Br was an effective bleach for smooth and uniform Ni, Co, and Ni–Co deposits due to the reduced grain sizes imposed by IL [21]. Likewise, [FPIM]Br, compared to [MOFIM]I, resulted in deposits with less improved morphology, obtaining an atomic radius of 51.1 nm, almost twice the atomic radius using [MOFIM]I (28 nm) [19]. In addition, there was a better inhibition efficiency, obtaining a Co content of up to 30 wt.%.

2.5. Copper

Due to its high electrical conductivity, copper is the most applicable metal in the electronics industry. In galvanizing processes, copper-based films have a wide application as an undercoat for other metallic finishes as they cover minor imperfections in the substrate [67,174]. Due to these properties, Cu electrodeposition is one of the preferred methods for introducing ILs into electrolyte solutions, second only to Al [100,109]. As with Al, the major Cu source for electrodeposition using ILs is metal chloride [32,175].

As with most studies with other metals, choline chloride-based ILs also promote a homogeneous, smooth, shiny, and corrosion-resistant deposit due to their ability to generate hydrophobicity on the metal surface [113,118]. However, the addition of nicotinic acid (NA) in the electrolyte can inhibit the electrochemical processes due to the formation of transient species near the electrode surface, influencing the nucleation kinetics and the faster growth of Cu deposits [140]. In contrast, sodium bromide modified the morphology of the deposits, not only of Cu, but also of Al, Sn, Ag, and Ni [136]. However, the electrochemical results did not indicate significant differences compared to the deposits formed by ChCl–EG without additives.

Recent studies highlight the use of Cu_2O as a source of Cu for its deposition under suitable dissolution conditions [100,112]. According to He et al. [112], Cu_2O dissolved in an electrolyte containing [EMIM]F–urea–H_2O at 353 K. Likewise, in another study, theu se of urea–EMIC as an electrolyte at 363 K increased the diffusion coefficient of the reaction to 1.02×10^{-10} m^2/s. In addition, urea–EMIC efficiently dissolved Cu_2O, improving the diffusion reaction, nuclei formation capacity, and Cu grain growth.

In contrast to pure copper deposition studies, for Cu–Pb alloys, the use of [Hbet][TFSA] promoted a complete dissolution of a mixture of water and CuO/PbO. The alloy morphology was altered by the nitrate reduction capacity [127] and the glucose oxidation [128]. Therefore, the system showed greater flexibility for electrocatalytic reduction or oxidation activities. The Cu–Sn alloy, popularly known as bronze, has good anti-corrosion properties. However, studies seek to improve the ratio of Cu:Sn using IL based on imidazolium cation, such as [Bmim]Cl [65,66], [EMIm]DCA [76], [EMIM]Cl [101], and [EMIm][TFSA] [114], with an Sn content of 13.7 at.% [65,66], 15 at.% [101], and 25 at.%, respectively [114].

In addition to improving anticorrosive properties, Jie et al. [65] reported that [BMIM]Cl in the Cu–Sn deposition system resulted in a crystalline plane (111). Due to the IL, the coloration became darker, making it interesting for industries that produce products with decorative aspects. The cyclic voltammetry peaks of Cu with [BMIM]Cl occur in two steps, 0.45~0.55 V for $Cu^{2+} \rightarrow Cu^{+}$ and 1.25~−1.5 V for $Cu^{+} \rightarrow Cu^{0}$, which could change the current density of the system during the process [65,66]. However, the reduction of the Cu–Sn alloy covered an intermediate reduction peak between −0.5 and −1.0 V, without interference in the alloy synthesis, with the reduction process occurring spontaneously and irreversibly. On the other hand, a system with [EMIm]DCA, polycarbonate membranes, and polystyrene models did not obtain a Cu–Sn alloy in the plane (111) [76]. The authors reported an oriented Cu_6Sn_5 alloy with nanofibers in the structure (221), being interesting for application in Li-ion batteries as anodic hosts.

2.6. Zinc

Zn is a low-cost material widely used in electroplating for application in the automotive and aerospace industries [176]. In addition, it has applications for energy storage due to the reversible capacity of its deposits [115,167]. However, the control of Zn alloys can be improved in terms of morphology [75], resulting in nanotubes [116]. In this context, IL-based electrolytes, instead of conventional aqueous-based electrolytes, have been promising in reducing harmful morphologies and forming a uniform metallic film.

The main dissolution of Zn for electrodeposition in ILs uses $ZnCl_2$ [17,80]. The IL control variables, such as viscosity, density, and conductivity for Zn electrodeposition, are analyzed with $ZnCl_2$ as the Zn source [27]. This control of the properties of an electrolyte containing ChCl–EG in a 1:2 ratio can result in Zn–Co alloys with corrosion resistivity up to 30 times higher than uncoated Cu [141]. ChCl–EG also improved charge transfer by agglomerating Zn–Ce alloy particles [142]. The Ce deposit occurred in cathodic and higher pH areas, demonstrating a tendency to improve the self-repair capacity of the alloy due to the Ce content.

Corrosion resistance was also evaluated for the ternary Zn–Mn–Sn alloy synthesized from an IL [143]. The control of the Sn content occurred due to the increase of the concentration and the potential. In addition, the ease of dissolution in Sn^{2+} and ChCl–EG improves the conductivity of the electrolyte solution. In this sense, both studies demonstrated the affinity of Zn and its alloys with ChCl–EG, encouraging the synthesis of new materials.

3. Electrodeposition of Light Metals (Li, Na, and Mg)

High reactivity is one of the main characteristics of light metals since a high oxidizing capacity impedes the formation of deposits. With the increase of studies in the field of catalytic reactions in batteries, the study of light metals deposition is increasing [111,177,178]. In this context, ILs are promising electrolyte agents due to their ability to stabilize the medium and expand the electrochemical windows, reaching potential values close to the redox potential of these metals.

For Li electrodeposition, IL influences the metal concentration profile as increasing concentration induces a drastic increase in electrolyte viscosity, resulting in a change in cell voltage [179]. Furthermore, these ILs can also change the roughness of the Li deposit [180], making them suitable electrolytes for second-generation batteries. Despite the difficulty of depositing this metal, TFSI and FSI are promising for this purpose due to the Li dissolution that occurs even at low concentrations of ILs [151].

He et al. [153] evaluated the combination of Li salt with bis(trifluoromethanesulfonyl)imide (TFSI) and bis(fluorosulfonyl)imide (FSI) for electrodeposition of Li on Cu using a solid electrolyte interphase (SEI) at lower overpotentials and in different proportions of IL. As the FSI concentration increased, the maximum current increased, and the maximum time decreased. In addition, there was a reduction in nucleation overpotentials with increasing FSI content, confirming the interfacial influence of SEI and the lower interfacial energy in the 0:1 TFSI:FSI ratio.

On the other hand, for Li electrodeposition on gold, the TFSI presented three distinct cathode peaks in the potential range from 0 to −2.5 V [152]. The first occurred in the potential region of the subpotential deposition (from −1.2 to −1.8 V), in which monatomic islands appeared with lengths between 300–370 pm. The second deposition occurred at potentials lower than −2.3 V, depositing a higher Li content. Finally, the third deposition at 0 V potential (related to Li growth) presented a uniform structure orientation (111).

In addition to battery applications, ILs also electrochemically extract these metals. For example, according to Zhang et al. [150], EC–$AlCl_3$ extracted Li from Li_2O for its subsequent deposition at 353 K, resulting in Al–Li nanosheets on the Al surface. For Mg, $[P_{4446}][NTf_2]$ acted as an excellent supporting electrolyte to resolve the electroconductivity of the weak polarity organic phase [156]. As a result, the electroconductivity of the organic phase was 254.5 μS cm^{-1} after extraction, facilitating the direct deposition of Mg.

4. Electrodeposition of Noble Metals

Noble metals (gold, silver, platinum, palladium, rhodium, ruthenium, iridium, and osmium) play a prominent role among metals. Except for Ag, they do not oxidize when exposed to the atmosphere. Due to their excellent physical and chemical properties, they are used in electroplating. Although electroplating processes focus on protecting the surface of metallic substrates against oxidation caused by aggressive agents, the process can only aim at the aesthetic and decorative aspects of the substrate. Likewise, despite the extensive exploitation of ILs for these metals, no studies were found regarding osmium as a deposit.

4.1. Silver

Although Ag has fewer alloys than gold, it is the most important noble metal for the electronics industry and commerce [117]. Furthermore, the use of Ag as a reversible metal in electrodeposition can promote energy savings, allow a low operating voltage, and provide excellent electrochemical stability [22]. However, the understanding of the early stages of Ag deposition and the investigation of process variables containing ILs is still preliminary.

Ehrenburg et al. [44] observed that deposition of Ag on a single crystal surface of Au(111) using [BMP][DCA] showed a stable deposit at room temperature. However, the potential modification altered the initial nucleation process, forming a pseudomorphic monolayer at ~40 mV subpotential. Sousa et al. [117] used [HMIM][HSO_4] as an electrolyte for silver deposition in a gold disc electrode. At room temperature, the results underscore a trend in using ILs in Ag deposits. However, the balance between Ag^+ cations and HSO_4^- anions limited the effect of temperature on deposition to values above 45 °C.

ILs in the nucleation and growth of Ag grains present in the main studies IL of low viscosity, mainly those containing dicyanamide anions and/or imidazolium cations, are being investigated [41,45,157]. According to Hou et al. [29], reversible electrochemical mirrors (REMs) using ILs of mono- and bis-imidazolium cations exhibited fast switching speeds, excellent cycling durability, small particle sizes, and uniform Ag nanoparticle films. However, bis-imidazoles have longer alkyl chains and higher charge densities, resulting in a more pronounced effect due to a greater reduction in grain size.

Another device of REMs was studied by Hou et al. [22]. The authors observed the influence of organic imidazolium cations on the switching speed and cycle durability according to the difference in adsorption energy. The higher this energy, the greater the adhesion between organic cations and Ag(111) surfaces. This strong adsorption would prevent aggregation and agglomeration during the nucleation of Ag nanoparticles, leading to a denser and more compact Ag film. The combination of fast switching and durable cycling stability allows adjustable windows based on Ag metal reversible electrodeposition and IL-based electrolytes, making REM devices a competitive and promising alternative to traditional smart-response materials.

Contrary to conventional REM devices, Yin et al. [53] studied a bistable electrochromic device (EC) that can reversibly transform transparent, mirror, and black states based on reversible Ag electrodeposition using [HBIm][Br]. The high viscosity of IL contributed to forming a barrier to bromide ions, protecting the Ag layer from dissolution in an open circuit. The studies of ILs for Ag electrodeposition for REM and EC devices with high-energy efficiency present a high potential for future investigations.

4.2. Gold

One of the most valuable noble metals, Au is widely used in areas such as biomedical, electronics, catalysis, and fuel cells due to its physicochemical properties [181]. In addition, due to continuous demand and a high and stable price, electroplating can be a lower-cost and less aggressive alternative for the environment for metal recovery, mainly for recycling and extraction of electronic equipment (e-waste) [182].

Au deposits with IL containing imidazolium cations show a high cathodic current efficiency during electrodeposition [28]. Yang et al. [28] proposed an aqueous biphasic

extraction (ABS) containing [EMIBr]. Phosphate-based salts were studied for Au(I) extraction from alkaline solutions of aurocyanide. Au recovery depended on the liquid (ionic) phase using electrodeposition at a controlled potential of −1.2 V at 298 K. More than 91.6% of Au(I) in the IL-rich solution was deposited without crystal formation of impurity. The studies discussed suggest that in Au deposition, ILs alone do not favor the acquisition of deposits. Therefore, other compounds are needed to form favorable interfaces for deposition. In contrast, a eutectic mixture of choline chloride with ethylene glycol in a 1:2 molar ratio resulted in an Au deposition efficiency of 30–70%.

Although the electrodeposition is selective, it does not present a high recovery of the metal since, for the same proportion, Ag with 99% purity was deposited [144]. However, using an active redox water–IL interface (RAIL), Au@Pd core-shell bimetallic nanofibers were obtained [183]. Furthermore, the automatic sequential reduction of $AuCl_4^-$ and $PdCl_4^{2-}$ at the IL–water interface was spontaneous for Au, which became the nucleus for the growth of Pd. Therefore, using RAILs for nanofiber synthesis may be applied to metal alloys.

4.3. Platinum

The other noble metals are platinum group metals, which comprise Pt, Pd, Rh, Ru, Os, and Ir. Due to its high hardness and low ability to perform chemical reactions, Pt has few alloys. Therefore, most IL and Pt studies are about extraction and separation with green solvents [48,122]. Although the extraction–electrodeposition system converts Pt(IV) into Pt(0), as displayed in Figure 4, the stripping system can also be applied in the same study.

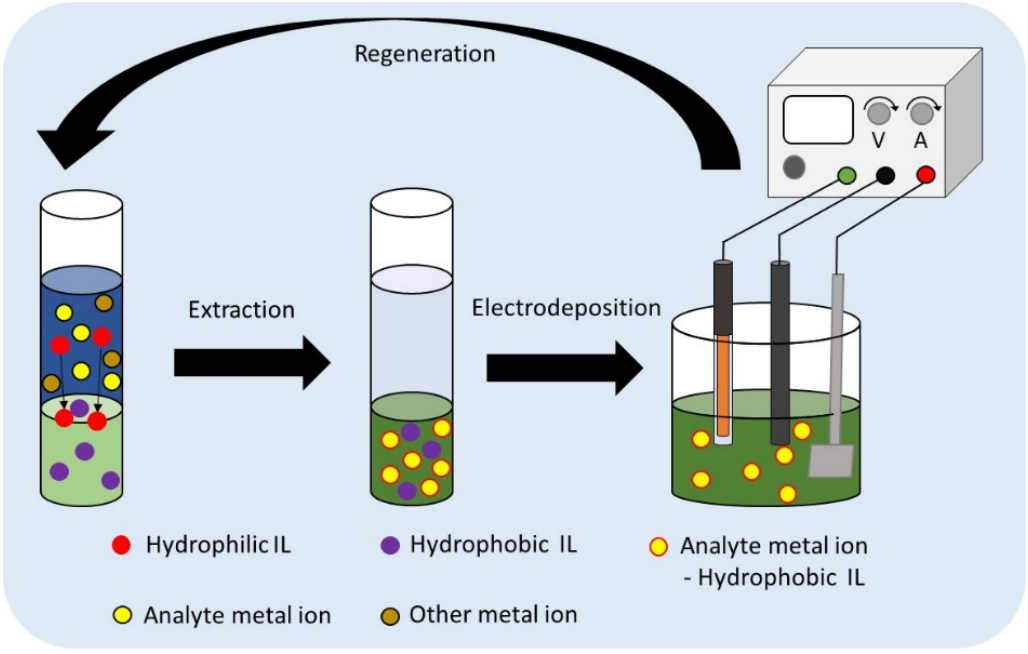

Figure 4. Extraction–electrodeposition process of metals in hydrophilic and hydrophobic ILs.

Chen et al. [121] studied five ILs of the imidazolium group: $[C_{12}PIm]Br$, $[C_{14}PIm]Br$, $[C_{16}PIm]Br$, $[C_{14}PImNH_2]Br$, and $[C_{14}BIm]Br$. After Pt extraction, the ILs were evaluated for electrodeposition on a Cu plate. The results showed that $[C_{14}PImNH_2]Br$ was the most efficient electrolyte in Pt deposition due to its hydrophobicity and greater alkyl chain in the imidazolium cation. Furthermore, in an acidic solution, the protonation of amino groups formed $–NH_3^+$ radicals that acted as additional binding sites for Pt(IV) and improved deposition efficiency as the concentration of $[C_{14}PImNH_2]Br$ increased. Likewise, another IL of imidazolium cation, [PAMI], was synthesized by radical polymerization with atom transfer, proving to be efficient for the nucleation and growth of Pt nanoparticles, leading to hydrogen evolution [31].

4.4. Palladium

As a member of the platinum group metals, Pd shares similar physical and mechanical attributes with the group. The electrodeposition of Pd using ILs has been increasing continuously, mainly in ILs of the imidazolium [103,104] and betatinium [110,131] groups. The studies highlight the ability of ILs to improve the diffusion coefficient of $PdCl_2$. This diffusion control is critical for controlled mass transfer at room temperature [104,107]. For [Emim]TA, the $PdCl_2$ diffusion coefficient increased with increasing temperature, and the diffusion activation energy was 43.66 kJ mol^{-1} [107].

Likewise, the electrodeposition of Pt has also been studied for extraction–electrodeposition systems and catalytic systems. The extraction–electrodeposition system was tested for some platinum group metals (Pd, Ru, and Rh), and the extraction was performed in HNO_3 for the phase ([Hbet][Tf_2N]) [131]. For potentials at −500, −600, and −750 mV vs. Fc/Fc^+, the deposition of the metals occurred only for Pd, with a yield of 99% and purity of 97%, demonstrating the ease of deposition of Pd in betatinium IL. In contrast, Shao et al. [110] obtained high recovery (90%) of Pd in an extraction system with mixed IL [C_8bet]Br/[C_4mim][NTf_2] at 348 K, demonstrating that ILs with different hydrophobicities allow electrodeposition at temperatures above ambient. The study also evaluated the stripping process for Pd with 1.2 M thiourea in 0.5 M HCl, obtaining a recovery above 91% even after repeating the extraction–electrodeposition–stripping process three times (Figure 5). The relationship between Pd and ILs is the most remarkable in the Pt group.

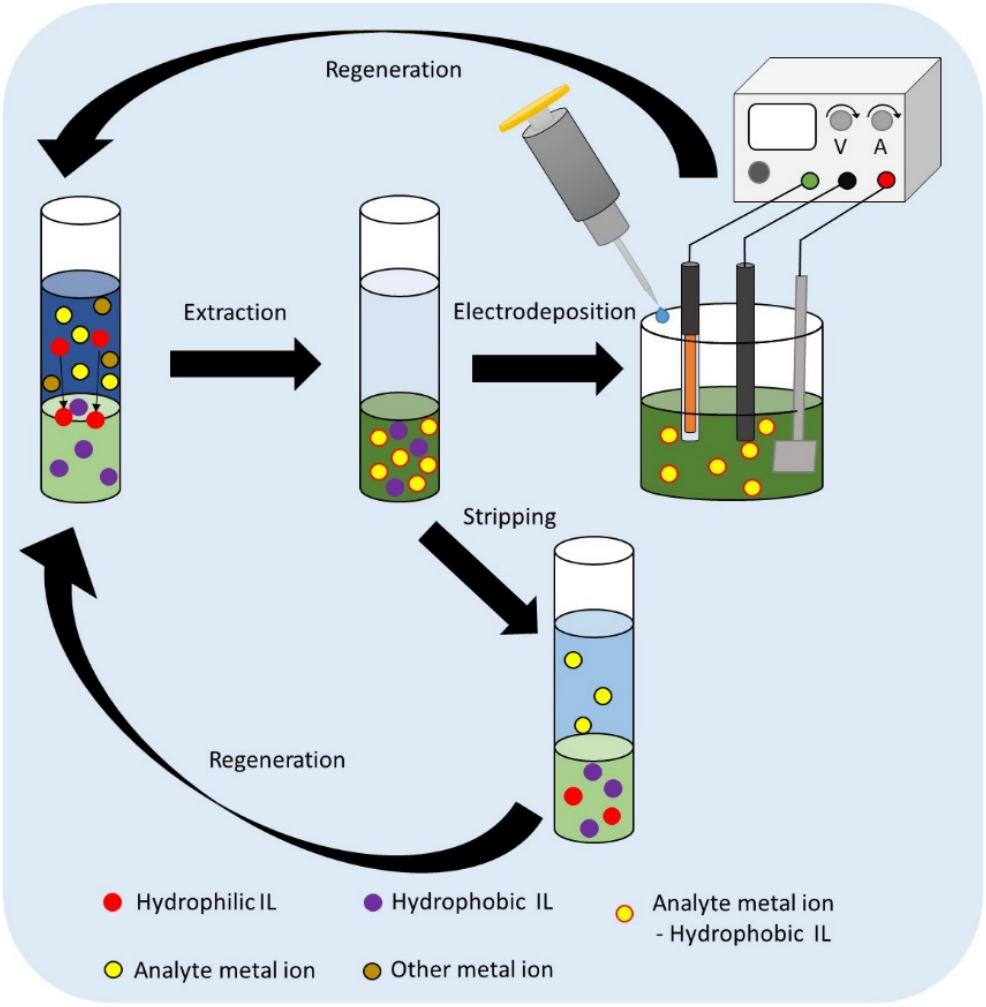

Figure 5. Metal extraction–electrodeposition process (with stripping) in hydrophilic and hydrophobic ILs.

As with Pt, Pd deposition was obtained on a polymer brush (PAMI) aimed at the hydrogen evolution reaction [31]. The polymer/metal-based hybrid structure favored the reaction. Furthermore, Pd deposition was efficient and similar to Pt. Jayanthi et al. [68] developed a fuel cell-based hydrogen amperometric sensor at room temperature. The sensor electrode was synthesized by electrodeposition of Pd with a carbon gas diffusion electrode in [C_4mim][Cl], obtaining a response range of the H_2 sensor at a concentration of 1 to 5%. On the other hand, in another approach, [C_4mim][Cl] was combined with ultrasonic wave-assisted electrodeposition for the deposition of an Ag–Pd alloy [64]. The process resulted in a catalyst with high electrocatalytic activity for the electro-oxidation of methanol and electro-reduction of hydrogen peroxide in an alkaline medium.

4.5. Rhodium, Ruthenium, and Iridium

The applications of electrodeposition using IL for the other platinum group metals are also explored with cations of the imidazolium group [73]. The principal purpose is for electrodeposition extraction, similar to those mentioned for the two previous elements of the group. For example, Song et al. [158] demonstrated that pH control was fundamental for extracting Ru from a solution containing Co and Cr. The solution components, di-(2-ethylhexyl)phosphoric acid (HDEHP) and IL [P_{2225}][TFSA], selectively removed Pd, aiming at electrodeposition.

Likewise, using the acid-IL system, García-Montoya et al. [160] promoted the reduction of Rh(III) to Rh in Cyphos IL 104® at a potential of −1.4 V. The stripping process after the electrodeposition showed high recovery rates. [Hbet][Tf_2N] promoted the extraction and deposition of only Pd, against Rh and Ru, in an HNO_3 phase to the ionic liquid phase [131]. However, the deposition was not efficient for Rh and Ru.

Regarding Ir extraction–electrodeposition, Ir(IV) can be reduced to Ir(0) at an optimal potential voltage of −1.72 V using [EBTOA]Br-Ir(IV)/[Bmim]PF_6 as the electrolyte. IL showed the potential to separate, deposit, and recover Ir from a mixed solution containing Pt(IV), Fe^{3+}, Al^{3+}, Cu^{2+}, Mg^{2+}, and Ca^{2+} at room temperature [70]. On the other hand, in the variation of the temperature range of 298–373 K, the same system promoted the reduction of Ir in two steps Ir(IV) + e^- → Ir(III) and Ir(III) + 3e^- → Ir(0) [71]. To assess the electrolyte lifetime, repeated electrodeposition resulted in a lifetime of up to 10 cycles for [EBTOA]Br-Ir(IV)/[Bmim]PF_6.

5. Electrodeposition of Rare Earth Metals

The 15 chemical elements of the lanthanide family and Yttrium are rare earth. These elements are made up of three distinct groups: (1) Light: lanthanum (La), cerium (Ce), praseodymium (Pr), and neodymium (Nd); (2) Middle: promethium (Pm), samarius (Sm), europium (Eu), and gadolinium (Gd); (3) Heavy: terbium (Tb), dysprosium (Dy), holmium (Ho), erbium (Er), thulium (Tm), ytterbium (Yb), lutetium (Lu), and yttrium (Y). They present an electronic structure in the 4f sublayer, conferring magnetic, optical, electrical, and catalytic properties. Their applications include the fields of energy production and storage [24]. However, a fundamental disadvantage of current processing methods includes the generation of toxic and radioactive waste. Therefore, new technologies can be explored to recover these metals by electrodeposition in more efficient electrolytes, such as ILs.

5.1. Light Rare Earth Metals

Among the light metals, there are fewer studies regarding La and Ce and ILs. For Ce, an alternative was to use [BMIm][BF_4] at temperatures above ambient. The IL had excellent applicability in the range of 343 to 373 K, resulting in a controlled diffusion process with a kinetic constant of 10^{-8} cm^2/s with homogeneous Ce deposits [74]. Another alternative was to include DMI–$LiNO_3$ as a support compound in the system, promoting the solvation of these compounds. The component formed ([Li(DMI)n]$^+$[NO_3]$^-$) favored the deposition of high-purity La on an Al substrate due to the NO_3^- anion preventing La solvation, highlighting the possibility of low-cost La extraction [24].

The $LiNO_3$ concentration significantly improves the conductivity of the system as the formation of nitrate anions reduces the solvation capacity of Nd, facilitating its electrodeposition [25]. Thus, Periyapperuma et al. [165] used $Nd(NO_3)\cdot 6H_2O$ as a source of Nd for electrodeposition on [C_4mpyr][DCA]. The low-cost, non-fluorinated IL showed that the innovation for a rare earth metal could be better exploited with another IL. Molodkina et al. [81] tried to deposit the Nd–Fe alloy with [EMIM][DCA]. However, at room temperature, the deposition of Nd and Fe, instead of the alloy, was prioritized due to the formation of an oxide/Nd hydroxide film. Only at 110 °C could IL cause a transition state (Fe*) in Fe which was capable of catalyzing the reduction of Nd^{3+} to Nd^0 through the magnetic properties of metals [106].

Pr alloys have also been approached with ILs for their separation and selective recovery in ore mixtures [36,147]. ChCl–UA reduced Pr^{3+}, Mg^{2+}, and Co^{2+} ions into a ternary Pr–Mg–Co alloy at a constant voltage of −1.15 V for 30 min [146]. Although the alloy presents amorphous morphology and contains cracks, its application may be important for alkaline solutions. On the other hand, the Pr–Mg–Ni alloy synthesized at −1.0 V for 20 min, despite also presenting an amorphous morphology, had reduced cracks [147]. The Pr–Mg–Ni alloy can be applied to saline and NaCl solutions. These studies with light rare earth metals alloys with ILs give new insight into recycling and targeting these compounds into protective films, providing a sustainable approach.

5.2. Medium and Heavy Rare Earth Metals

There are fewer studies for medium and heavy rare earth metals involving ILs than light metals. However, the [BMP][DCA] stands out for electrodeposition of medium rare earth metals. With this IL, the electrochemical windows of electroreduction from the Eu^{2+} ion to Eu^0 increased compared to a greater amount of water in the medium [42]. It was also interesting to reduce Sm in two steps, from Sm^{3+} to Sm^{2+} and Sm^{2+} to Sm^0 at room temperature, demonstrating control of diffusional transfer outside the high temperatures (323–373 K) studied with other electrolytes [39].

For heavy metals, the molten salt electrolysis process followed by electrodeposition improved with the addition of BMPyOTf, allowing the electrodeposition of Dy [46]. However, the reduction was obtained at more positive potentials by adding water (−3.3 V without water and −2.4 V with water). In addition to decreasing the reduction of thermodynamics, the introduction of water also improves nucleation, deposition rate, and faradaic efficiency [51].

6. Electrodeposition with Other Metals

Electrodeposition of metals such as gallium (Ga), chromium (Cr), tellurium (Te), tin (Sn), and others [37,38,162] are difficult to discuss due to the difficulty in the reduction process of the element on a compatible surface [14]. Therefore, although ILs have high electrochemical windows and good stability in electron transfer, only some studies addressed this series of metals, challenging the expansion of studies of ILs as electrolytes controlling electrodeposition.

The passivation of Cr and substrate during deposition made it additional Cr deposition and its anodic dissolution difficult [43]. Therefore, the authors' objective in the study was to deposit Cr with dicyanamide anions. In another study, Bakkar et al. [102] deposited Ga with anhydrous aluminum chloride ($AlCl_3$) and EMIC. However, the deposit did not show a well-developed homogeneous microstructure through the progressive nucleation-growth mechanism, making it difficult to relate the deposit to a controlled diffusion process. On the other hand, Hsieh et al. [40] presented a controlled diffusion process for a Ga-Sb alloy using [BMP][DCA].

Another metal deposited together with alloys is Sn. According to Shi et al. [148], choline–urea chloride allowed the synthesis of ternary Sn–Co–Ni and Sn–Co–Zn alloys with morphologies influenced by potential. As the potential increased, the Sn–Co–Ni alloy changed from needle-shaped crystals to a three-dimensional structure. In contrast, the

Sn–Co–Zn alloy changed its morphology from cubic crystals to flower-shaped particles, reinforcing that ILs exert control over the deposition of these metals and their alloys.

The ability of ILs to dissolve the salts or oxides of these uncommon metals is remarkable, since obtaining the deposit allows a selective separation of elements in a solution containing other metals. [Hbet][TFSA] dissolved PbO and PbO_2, resulting in smooth, uniform, and crystalline deposits [130]. Furthermore, this IL allowed the electrochemical extraction of Pb from several water-insoluble Pb compounds. In another study, [Bmim][Ac] at 90 °C showed advantages such as low vapor pressure, wide electrochemical window, and good ionic mobility to dissolve $Cd(CH_3COO)_2$ (anhydrous) and TeO_2 and form a Cd–Te alloy in a constant potential of −1.20 V [50].

7. Patents and Future Perspectives

Most of the patented studies on the subject of metal electrodeposition involving ionic liquids are simple. The processes show fast electrodeposition speed, and are environmentally friendly, safe, reliable, and non-toxic, in addition to the formation of a homogeneous deposit [184–188]. Other more sophisticated patents explore systems that involve the catalytic evolution of hydrogen [189] and oxygen [190] for the deposition of hard-to-obtain alloys.

Patents using cations of the imidazole group also stand out for the electrodeposition of metals [191–193]. Using the imidazole IL, promoting direct electrolytic oxidation of zinc on stainless steel (or copper) sheet resulted in a Zn yield of up to 99% [191]. In another invention [184], the authors identified the organic cations of tetraalkylammonium, 1-alkyl-3-methyl imidazolium, 1-alkylpyridinium, N-methyl-N-alkylpyrrolidinium, trialkylsulfonium or tetraalkylphosphonium were essential for the deposition of alkali metals, allowing applications for vapor cells used in optical magnetometry and atomic clocks. The number of patents involving catalytic systems and electrodeposition shows a growth trend and exploration of inventions associated with these techniques. However, as described in this review, no studies were observed that explore the extraction–electrodeposition system. Therefore, inventions in this field could be developed involving ILs.

8. Conclusions

This review discussed the variety of metals and their alloys considering IL-based electrolytes. In recent years, there has been an increase in the number of studies related to electrodeposition with ILs. They increase the mass transfer rate and improve control of the nucleation process and deposit grain growth. The morphology of most common metals is homogeneous and smooth when synthesized with ILs. For heterogeneous deposits, some ILs modify this morphology, such as choline ethylene glycol chloride, choline urea chloride, BMIC, and others. However, the morphology can be nodular for some noble metals including Pt, Pd, and Co. This nodular surface also occurs in the alloys of these metals.

For common metals, the proportion of IL with the metal source strongly influences the diffusion process, facilitating the control of nucleation and grain growth. It should be noted that Al is the most common metal for electrodeposition with ILs. Parameters such as current density and temperature can also interfere with the deposition of these metals, highlighting systems with temperatures mostly below 100 °C, one of the advantages of ILs. In light metals, catalytic systems involving Li batteries stand out with ILs of wide electrochemical windows, reaching the redox potential of these metals, allowing efficient electrodeposition. Furthermore, extraction–electrodeposition systems with ILs that have different hydrophobicities are effective for noble metals contained in a complex mixture. This technology could be exploited for other metals and rare earth. Likewise, the ability to dissolve metal oxides and salts is also crucial for applying ILs. In this way, it is expected that ILs will continue to present significant applications in the biological, chemical, and energy areas.

Author Contributions: Conceptualization, J.G.d.R.d.C. and J.M.C.; methodology, J.G.d.R.d.C. and J.M.C.; formal analysis, J.G.d.R.d.C.; investigation, J.G.d.R.d.C.; resources, A.F.d.A.N.; writing—original draft preparation, J.G.d.R.d.C.; writing—review and editing, J.M.C. and A.F.d.A.N.; visualization, J.G.d.R.d.C. and J.M.C.; supervision, A.F.d.A.N.; project administration, A.F.d.A.N.; funding acquisition, A.F.d.A.N. All authors have read and agreed to the published version of the manuscript.

Funding: This study was financed in part by the Coordenação de Aperfeiçoamento de Pessoal de Nível Superior-Brasil (CAPES)-Finance Code 001.

Data Availability Statement: Not applicable.

Conflicts of Interest: The authors declare no conflict of interest.

References

1. Djokic, S.S. *Electrodeposition—Theory and Practice*, 1st ed.; Springer: New York, NY, USA, 2010; p. XVII-295.
2. Gamburg, Y.D.; Zangari, G. *Theory and Practice of Metal Electrodeposition*, 1st ed.; Springer: New York, NY, USA, 2011; p. XVII-378.
3. Kaur, G.; Kumar, H.; Singla, M. Diverse applications of ionic liquids: A comprehensive review. *J. Mol. Liq.* **2022**, *351*, 118556. [CrossRef]
4. Lebedeva, O.; Kultin, D.; Zakharov, A.; Kustov, L. Advances in application of ionic liquids: Fabrication of surface nanoscale oxide structures by anodization of metals and alloys. *Surf. Interfaces* **2022**, *34*, 102345. [CrossRef]
5. Maniam, K.K.; Paul, S. A Review on the Electrodeposition of Aluminum and Aluminum Alloys in Ionic Liquids. *Coatings* **2021**, *11*, 80. [CrossRef]
6. Tiago, G.A.O.; Matias, I.A.S.; Ribeiro, A.P.C.; Martins, L.M.D.R.S. Application of Ionic Liquids in Electrochemistry—Recent Advances. *Molecules* **2020**, *25*, 5812. [CrossRef] [PubMed]
7. Welton, T. Ionic liquids: A brief history. *Biophys. Rev.* **2018**, *10*, 691–706. [CrossRef]
8. Zhou, J.; Sui, H.; Jia, Z.; Yang, Z.; He, L.; Li, X. Recovery and purification of ionic liquids from solutions: A review. *RSC Adv.* **2018**, *8*, 32832–32864. [CrossRef]
9. Dołżonek, J.; Kowalska, D.; Maculewicz, J.; Stepnowski, P. Regeneration, Recovery, and Removal of Ionic Liquids. In *Encyclopedia of Ionic Liquids*; Zhang, S., Ed.; Springer: Singapore, 2020; pp. 1–9.
10. Quijada-Maldonado, E.; Olea, F.; Sepúlveda, R.; Castillo, J.; Cabezas, R.; Merlet, G.; Romero, J. Possibilities and challenges for ionic liquids in hydrometallurgy. *Sep. Purif. Technol.* **2020**, *251*, 117289. [CrossRef]
11. Zhang, M.; Peng, D.; Peng, F.; Huang, A.; Song, K.; He, Q.; Yin, C.; Rao, J.; Zhang, Y.; Chen, H.; et al. Effects of Additives Containing Cyanopyridine on Electrodeposition of Bright Al Coatings from $AlCl_3$-EMIC Ionic Liquids. *Coatings* **2021**, *11*, 1396. [CrossRef]
12. Yavuz, A.; Ozdemir, N.; Yilmaz Erdogan, P.; Zengin, H.; Zengin, G.; Bedir, M. Effect of electrodeposition potential and time for nickel film generation from ionic liquid electrolytes for asymmetric supercapacitor production. *Thin Solid Film.* **2020**, *711*, 138309. [CrossRef]
13. Li, W.; Hao, J.; Liu, W.; Mu, S. Electrodeposition of nano Ni–Co alloy with (220) preferred orientation from choline chloride-urea: Electrochemical behavior and nucleation mechanism. *J. Alloy. Compd.* **2021**, *853*, 157158. [CrossRef]
14. Sides, W.D.; Huang, Q. Electrodeposition of manganese thin films on a rotating disk electrode from choline chloride/urea based ionic liquids. *Electrochim. Acta* **2018**, *266*, 185–192. [CrossRef]
15. Li, W.; Hao, J.; Mu, S.; Liu, W. Electrochemical behavior and electrodeposition of Ni-Co alloy from choline chloride-ethylene glycol deep eutectic solvent. *Appl. Surf. Sci.* **2020**, *507*, 144889. [CrossRef]
16. Alesary, H.F.; Cihangir, S.; Ballantyne, A.D.; Harris, R.C.; Weston, D.P.; Abbott, A.P.; Ryder, K.S. Influence of additives on the electrodeposition of zinc from a deep eutectic solvent. *Electrochim. Acta* **2019**, *304*, 118–130. [CrossRef]
17. Bakkar, A.; Neubert, V. Recycling of cupola furnace dust: Extraction and electrodeposition of zinc in deep eutectic solvents. *J. Alloys Compd.* **2019**, *771*, 424–432. [CrossRef]
18. Wang, S.; Zou, X.; Lu, Y.; Rao, S.; Xie, X.; Pang, Z.; Lu, X.; Xu, Q.; Zhou, Z. Electrodeposition of nano-nickel in deep eutectic solvents for hydrogen evolution reaction in alkaline solution. *Int. J. Hydrog. Energy* **2018**, *43*, 15673–15686. [CrossRef]
19. Omar, I.M.A.; Aziz, M.; Emran, K.M. Part I: Ni-Co alloy foils electrodeposited using ionic liquids. *Arab. J. Chem.* **2020**, *13*, 7707–7719. [CrossRef]
20. Omar, I.M.A.; Al-Fakih, A.M.; Aziz, M.; Emran, K.M. Part II: Impact of ionic liquids as anticorrosives and additives on Ni-Co alloy electrodeposition: Experimental and DFT study. *Arab. J. Chem.* **2021**, *14*, 102909. [CrossRef]
21. Omar, I.M.A.; Aziz, M.; Emran, K.M. Impact of ionic liquid [FPIM]Br on the electrodeposition of Ni and Co from an aqueous sulfate bath. *J. Mater. Res. Technol.* **2021**, *12*, 170–185. [CrossRef]
22. Hou, X.; Wang, Z.; Pan, J.; Yan, F. Ionic Liquid Electrolyte-Based Switchable Mirror with Fast Response and Improved Durability. *ACS Appl. Mater. Interfaces* **2021**, *13*, 37339–37349. [CrossRef]
23. Zhang, X.; Liu, A.; Liu, F.; Shi, Z.; Zhang, B.; Wang, X. Electrodeposition of aluminum–magnesium alloys from an aluminum-containing solvate ionic liquid at room temperature. *Electrochem. Commun.* **2021**, *133*, 107160. [CrossRef]

24. Zhang, B.; Yao, Y.; Shi, Z.; Xu, J.; Liu, Y.; Wang, Z. Communication—Direct Room-Temperature Electrodeposition of La from $LaCl_3$ in an Organic Solvent Supported by $LiNO_3$. *J. Electrochem. Soc.* **2019**, *166*, D218. [CrossRef]
25. Zhang, B.; Wang, L.; Pan, K.; Zhang, W.; Liu, Y.; Zhang, Y.; Zhang, L.; Shi, Z. $LiNO_3$-Supported Electrodeposition of Metallic Nd from Nd-Containing Solvate Ionic Liquid. *J. Phys. Chem. C* **2021**, *125*, 20798–20805. [CrossRef]
26. Liu, A.-M.; Yao, Y.; Guo, M.-X.; Liu, Y.-B.; Shi, Z.-N.; Liu, F.-G.; Hu, X.-W.; He, W.-C.; Wang, Z.-W. Physicochemical properties of DMI–$LiNO_3$ solvated ionic liquid and its application in electrodeposition of neodymium at room temperature. *Trans. Nonferrous Met. Soc. China* **2021**, *31*, 2522–2531. [CrossRef]
27. Liu, A.-M.; Guo, M.-X.; Shi, Z.-N.; Liu, Y.-B.; Liu, F.-G.; Hu, X.-W.; Yang, Y.-J.; Tao, W.-J.; Wang, Z.-W. Physicochemical properties of 1,3-dimethyl-2-imidazolinone−$ZnCl_2$ solvated ionic liquid and its application in zinc electrodeposition. *Trans. Nonferrous Met. Soc. China* **2021**, *31*, 832–841. [CrossRef]
28. Yang, X.; Miao, C.; Sun, Y.; Lei, T.; Xie, Q.; Wang, S. Efficient extraction of gold(I) from alkaline aurocyanide solution using green ionic liquid-based aqueous biphasic systems. *J. Taiwan Inst. Chem. Eng.* **2018**, *91*, 176–185. [CrossRef]
29. Hou, X.; Wang, Z.; Zheng, Z.; Guo, J.; Sun, Z.; Yan, F. Poly(ionic liquid) Electrolytes for a Switchable Silver Mirror. *ACS Appl. Mater. Interfaces* **2019**, *11*, 20417–20424. [CrossRef]
30. Chunyan, L.; Nishikawa, K.; Moon, J.; Kanamura, K. Electrodeposition of Zn from 1–allyl–3–methylimidazolium bromide containing $ZnBr_2$. *J. Electroanal. Chem.* **2019**, *832*, 467–474. [CrossRef]
31. Pham-Truong, T.-N.; Mebarki, O.; Ranjan, C.; Randriamahazaka, H.; Ghilane, J. Electrochemical Growth of Metallic Nanoparticles onto Immobilized Polymer Brush Ionic Liquid as a Hybrid Electrocatalyst for the Hydrogen Evolution Reaction. *ACS Appl. Mater. Interfaces* **2019**, *11*, 38265–38275. [CrossRef]
32. Ezawa, K.; Nishi, N.; Sakka, T. In-situ electrochemical SPR study of gold surface smoothing by repetitive cathodic deposition and anodic dissolution of copper in an ionic liquid. *J. Electroanal. Chem.* **2020**, *877*, 114611. [CrossRef]
33. Manjum, M.; Serizawa, N.; Katayama, Y. Electrodeposition of Co in an Amide-Type Ionic Liquid under an External Magnetic Field. *J. Electrochem. Soc.* **2021**, *168*, 042504. [CrossRef]
34. Chen, Y.-T.; Li, C.-H.; Chen, P.-Y. Galvanic displacement on electrodeposited tangled Zn nanowire sacrificial template for preparing porous and hollow Ni electrodes in ionic liquid. *J. Mol. Liq.* **2020**, *298*, 112050. [CrossRef]
35. Ismail, A.S. Electrodeposition of aluminium–copper alloy from 1-butyl-1-methylpyrrolidinium bis(trifluoromethylsulfonyl) imide ionic liquid. *Egypt. J. Pet.* **2017**, *26*, 61–65. [CrossRef]
36. Jürjo, S.; Oll, O.; Paiste, P.; Külaviir, M.; Zhao, J.; Lust, E. Electrochemical co-reduction of praseodymium and bismuth from 1-butyl-1-methylpyrrolidinium bis(fluorosulfonyl)imide ionic liquid. *Electrochem. Commun.* **2022**, *138*, 107285. [CrossRef]
37. Wu, Q.; Pulletikurthi, G.; Carstens, T.; Endres, F. On the Electrodeposition of Titanium from TiCl4 in 1-butyl-1-methylpyrrolidinium bis(trifluoromethylsulfonyl)amide: In Situ AFM and Spectroscopic Investigations. *J. Electrochem. Soc.* **2018**, *165*, D223. [CrossRef]
38. Simunkova, H.; Lednický, T.; Whitehead, A.H.; Kalina, L.; Simunek, P.; Hubalek, J. Tantalum-based nanotube arrays via porous-alumina-assisted electrodeposition from ionic liquid: Formation and electrical characterization. *Appl. Surf. Sci.* **2021**, *548*, 149264. [CrossRef]
39. Andrew, C.; Murugesan, C.; Jayakumar, M. Electrochemical Behavior of Sm(III) and Electrodeposition of Samarium from 1-Butyl-1-Methylpyrrolidinium Dicyanamide Ionic Liquid. *J. Electrochem. Soc.* **2022**, *169*, 022503. [CrossRef]
40. Hsieh, Y.-T.; Liu, Y.-C.; Lo, N.-C.; Lin, W.-J.; Sun, I.W. Electrochemical co-deposition of gallium and antimonide from the 1-butyl-1-methylpyrrolidinium dicyanamide room temperature ionic liquid. *J. Electroanal. Chem.* **2019**, *832*, 48–54. [CrossRef]
41. Molodkina, E.B.; Ehrenburg, M.R.; Broekmann, P.; Rudnev, A.V. Initial stages of silver electrodeposition on single crystal electrodes from ionic liquids. *Electrochim. Acta* **2019**, *299*, 320–329. [CrossRef]
42. Ehrenburg, M.R.; Molodkina, E.B.; Mishchenko, A.; Rudnev, A.V. The promoting effect of water on the electrodeposition of Eu in a dicyanamide ionic liquid. *Electrochim. Acta* **2021**, *379*, 138169. [CrossRef]
43. Molodkina, E.B.; Ehrenburg, M.R.; Broekmann, P.; Rudnev, A.V. Electrodeposition of chromium on single-crystal electrodes from solutions of Cr(II) and Cr(III) salts in ionic liquids. *J. Electroanal. Chem.* **2020**, *860*, 113892. [CrossRef]
44. Ehrenburg, M.R.; Molodkina, E.B.; Broekmann, P.; Rudnev, A.V. Underpotential Deposition of Silver on Au(111) from an Air- and Water-Stable Ionic Liquid Visualized by In-Situ STM. *ChemElectroChem* **2019**, *6*, 1149–1156. [CrossRef]
45. Rahali, S.; Zarrougui, R.; Marzouki, M.; Ghodbane, O. Electrodeposition of silver from the ionic liquid Butylpyridinium dicyanamide. *J. Electroanal. Chem.* **2020**, *871*, 114289. [CrossRef]
46. Atifi, A.; Baek, D.L.; Fox, R.V. Electrodeposition of Dysprosium in pyrrolidinium triflate ionic liquid at ambient temperature: Unraveling system efficiency and impact of solvation interplays on the reduction process. *Electrochim. Acta* **2021**, *378*, 138140. [CrossRef]
47. Lambri, O.A.; Weidenfeller, B.; Bonifacich, F.G.; Pulletikurthi, G.; Xu, J.; Weidenfeller, L.; Endres, F. Damping of Fe-Al alloy electrodeposited in an ionic liquid. *Mat. Res.* **2018**, *21*, e20170805. [CrossRef]
48. Liu, W.; Wang, Q.; Zheng, Y.; Wang, S.; Yan, Y.; Yang, Y. Extraction behaviour and mechanism of Pt(iv) and Pd(ii) by liquid–liquid extraction with an ionic liquid [HBBIm]Br. *Dalton Trans.* **2017**, *46*, 7210–7218. [CrossRef]
49. He, X.; Zhang, C.; Zhu, Q.; Lu, H.; Cai, Y.; Wu, L. Electrodeposition of Nanocrystalline Ni-Fe Alloy Coatings Based on 1-Butyl-3-Methylimidazolium-Hydrogen Sulfate Ionic Liquid. *J. Nanosci. Nanotechnol.* **2017**, *17*, 1108–1115. [CrossRef]
50. Waldiya, M.; Bhagat, D.; Mukhopadhyay, I. Electrodeposition of CdTe thin film from acetate-based ionic liquid bath. *AIP Conf. Proc.* **2018**, *1961*, 030048. [CrossRef]

51. Orme, K.; Baek, D.L.; Fox, R.V.; Atifi, A. Water Interplays during Dysprosium Electrodeposition in Pyrrolidinium Ionic Liquid: Deconvoluting the Pros and Cons for Rare Earth Metallization. *ACS Sustain. Chem. Eng.* **2021**, *9*, 14631–14643. [CrossRef]
52. Maizi, R.; Meddour, A.; Rousse, C. Structural and electrochemical properties of thin layers of binary Ni-Fe alloys electrodeposited by two different baths: Acid and ionic liquid. *Surf. Rev. Lett.* **2017**, *25*, 1950025. [CrossRef]
53. Yin, Y.; Zhu, H.; Wu, T.; Liao, P.; Lan, C.; Li, C. Bistable Silver Electrodeposition-Based Electrochromic Device with Reversible Three-State Optical Transformation By Using WO_3 Nanoislands Modified ITO Electrode. *Adv. Mater. Interfaces* **2022**, *9*, 2102566. [CrossRef]
54. Peng, Y.; Shinde, P.S.; Reddy, R.G. Diffusion coefficient and nucleation density studies on electrochemical deposition of aluminum from chloroaluminate ionic liquid electrolytes. *J. Electroanal. Chem.* **2021**, *895*, 115363. [CrossRef]
55. Zhang, D.; Mu, Y.; Li, H.; Yang, Z.; Yang, Y. A new method for electrodeposition of Al coatings from ionic liquids on AZ91D Mg alloy in air. *RSC Adv.* **2018**, *8*, 39170–39176. [CrossRef]
56. Caporali, S.; Martinuzzi, S.M.; Von Czarnecki, P.; Schubert, T.J.S.; Bardi, U. Effects of Metal Ions on the Aluminum Electrodeposition from Ionic Liquids. *J. Mater. Eng. Perform.* **2017**, *26*, 685–691. [CrossRef]
57. Peng, Y.; Shinde, P.; Reddy, R.G. Nucleation Study on Deposition of Aluminum from 1-Butyl-3-Methylimidazolium Chloride and Aluminum Chloride Ionic Liquid Electrolyte. *ECS Trans.* **2020**, *98*, 199. [CrossRef]
58. Wang, Y.; Reddy, R.G.; Wang, R. Dendrite-free Al recycling via electrodeposition using ionic liquid electrolytes: The effects of deposition temperature and cathode surface roughness. *J. Clean. Prod.* **2021**, *287*, 125043. [CrossRef]
59. Lang, H.; Wang, Q.; Tu, X.; Chen, S. Template-free preparation of spherical Al particles in aluminum chloride and 1-butyl-3-methylimidazolium chloride ionic liquid. *Ionics* **2018**, *24*, 1781–1788. [CrossRef]
60. Zhou, J.; Zheng, X.; Li, J.; Li, X.; Lu, K. Electrodeposited Al mesocrystal with high thermal stability and high hardness. *Scr. Mater.* **2022**, *221*, 114964. [CrossRef]
61. Tian, G.-C.; Yuan, Q.-X. Effect of dichloromethane and toluene on the structure, property, and Al electrodeposition in 1-butyl-3-methylimidazolium chloroaluminate ionic liquid. *Chin. J. Eng.* **2021**, *43*, 1037. [CrossRef]
62. Xu, C.; Hua, Y.; Zhang, Q.; Li, J.; Lei, Z.; Lu, D. Electrodeposition of Al-Ti alloy on mild steel from AlCl3-BMIC ionic liquid. *J. Solid State Electrochem.* **2017**, *21*, 1349–1356. [CrossRef]
63. Shinde, P.S.; Peng, Y.; Reddy, R.G. Potentiostatic Electrodeposition of Ti–Al Alloy with 40% Titanium from the Lewis Acidic 1-Butyl-3-Methylimidazolium Chloride-Aluminum Chloride Ionic Liquid Electrolyte. In *TMS 2022 151st Annual Meeting & Exhibition Supplemental Proceedings*; Springer International Publishing: Cham, Switzerland, 2022; pp. 74–86.
64. Sriram, P.; Kumar, M.K.; Selvi, G.T.; Jha, N.S.; Mohanapriya, N.; Jha, S.K. Elucidation of ultrasonic wave-assisted electrodeposited AgPd nanoalloy from ionic liquid as an efficient bifunctional electrocatalyst for methanol oxidation and hydrogen peroxide reduction. *Electrochim. Acta* **2019**, *323*, 134809. [CrossRef]
65. Sun, J.; Ming, T.-Y.; Qian, H.-X.; Li, Q.-S. Preparation of black Cu-Sn alloy with single phase composition by electrodeposition method in 1-butyl-3-methylimidazolium chloride ionic liquids. *Mater. Chem. Phys.* **2018**, *219*, 421–424. [CrossRef]
66. Sun, J.; Ming, T.Y.; Qian, H.X.; Li, Q.S. Electrochemical behaviors and electrodeposition of single-phase Cu-Sn alloy coating in [BMIM]Cl. *Electrochim. Acta* **2019**, *297*, 87–93. [CrossRef]
67. Sun, J.; Ming, T.-Y.; Qian, H.-X.; Li, Q.-S. Preparation of copper–silver alloy with different morphologies by a electrodeposition method in 1-butyl-3-methylimidazolium chloride ionic liquid. *Bull. Mater. Sci.* **2019**, *42*, 227. [CrossRef]
68. Jayanthi, E.; Murugesan, N.; Suneesh, A.S.; Ramesh, C.; Anthonysamy, S. Sensing Behavior of Room Temperature Amperometric H_2 Sensor with Pd Electrodeposited from Ionic Liquid Electrolyte as Sensing Electrode. *J. Electrochem. Soc.* **2017**, *164*, H5210. [CrossRef]
69. Hallaj, R.; Mohammadian, N.; Ghaderi, S.; Navaee, A. Nonenzymatic and low potential glucose sensor based on electrodeposited Ru-nanofilm from ionic liquid electrolyte. *Mater. Sci. Eng. B* **2020**, *261*, 114666. [CrossRef]
70. Fan, M.; Li, S.; Deng, H.; Zhang, X.; Luo, G.; Huang, Z.; Chen, M. Separation and recovery of iridium(IV) from simulated secondary resource leachate by extraction—Electrodeposition. *Sep. Purif. Technol.* **2022**, *289*, 120765. [CrossRef]
71. Matsumiya, M.; Kinoshita, R.; Tsuchida, Y.; Sasaki, Y. Recovery of Iridium by Solvent Extraction and Direct Electrodeposition Using Phosphonium-Based Ionic Liquids. *J. Electrochem. Soc.* **2021**, *168*, 056501. [CrossRef]
72. Ries, L.A.d.S.; de Brito, H.A.; Gasparin, F.P.; Muller, I.L. Additive-free electrodeposition of cobalt on silicon from 1-butyl-3-methylimidazolium tetrafluoroborate ionic liquid. *J. Mol. Liq.* **2021**, *325*, 114787. [CrossRef]
73. Qian, J.; Li, X.; Luan, H.; Li, T.; Yin, Y. Electrodeposition of Iridium in 1-Butyl-3-Methylimidazolium Tetrafluoroborate Ionic Liquid. *Rare Met. Mater. Eng.* **2017**, *46*, 1756–1761. [CrossRef]
74. Chen, L.; Li, Y.; Shi, X.; Wang, D.; Wang, G.; Jiao, C.; Zhang, M. Electrochemical properties of Ln(III) (Ln = Ce, Gd) in 1-butyl-3-methylimidazolium tetrafluoroborate ionic liquid. *J. Radioanal. Nucl. Chem.* **2021**, *329*, 1269–1276. [CrossRef]
75. Keist, J.S.; Hammons, J.A.; Wright, P.K.; Evans, J.W.; Orme, C.A. Coupling in situ atomic force microscopy (AFM) and ultra-small-angle X-ray scattering (USAXS) to study the evolution of zinc morphology during electrodeposition within an imidazolium based ionic liquid electrolyte. *Electrochim. Acta* **2020**, *342*, 136073. [CrossRef]
76. Elbasiony, A.M.; Prowald, A.; Abedin, S.Z.E.; Endres, F. Electrochemical synthesis of nanowires and macroporous CuSn alloy from ionic liquids. *J. Solid State Electrochem.* **2022**, *26*, 783–789. [CrossRef]
77. Mardani, R.; Shahmirzaee, H.; Ershadifar, H.; Vahdani, M.R. Electrodeposition of $Ni_{32}Fe_{48}Mo_{20}$ and $Ni_{52}Fe_{33}W_{15}$ alloy film on Cu microwire from ionic liquid containing plating bath. *Surf. Coat. Technol.* **2017**, *324*, 281–287. [CrossRef]

78. Jesmani, S.M.; Amini, R.; Abdollah-Pour, H.; Mohammadian-Semnani, H. Effect of current density on Ni-Mo electrodeposition using EMIM [Br]. *Surf. Eng.* **2019**, *35*, 1088–1096. [CrossRef]
79. Jesmani, S.M.; Mohammadian-Semnani, H.; Abdollah-Pour, H.; Amini, R. The effect of pH on electrocatalytic properties of electrodeposited Ni–Mo/Ni coating using 1-ethyl-3-methylimidazolium bromide. *Mater. Res. Express* **2019**, *6*, 1065e1062. [CrossRef]
80. Yang, J.-M.; Hsieh, Y.-T.; Chu-Tien, T.-T.; Sun, I.W. Electrodeposition of Distinct One-Dimensional Zn Biaxial Microbelt from the Zinc Chloride-1-Ethyl-3-methylidazolium Chloride Ionic Liquid. *J. Electrochem. Soc.* **2011**, *158*, D235. [CrossRef]
81. Molodkina, E.B.; Ehrenburg, M.R.; Arkhipushkin, I.A.; Rudnev, A.V. Interfacial effects in the electro(co)deposition of Nd, Fe, and Nd-Fe from an ionic liquid with controlled amount of water. *Electrochim. Acta* **2021**, *398*, 139342. [CrossRef]
82. Xu, D.; Li, J.; Liang, C.; Liu, J.; Wang, H.; Ling, G. Increasing anhydrous chromium chloride concentration in AlCl3–EMIC ionic liquid: A step towards non-hydrogen-embrittlement chromium electroplating. *RSC Adv.* **2022**, *12*, 1855–1861. [CrossRef]
83. Farisi, M.S.A.; Hertel, S.; Wiemer, M.; Otto, T. Investigation of aluminum patterned electrodeposition process from $AlCl_3$-[EMIm]Cl ionic liquid for microsystems application. In Proceedings of the 2018 International Conference on Electronics Packaging and iMAPS All Asia Conference (ICEP-IAAC), Mie, Japan, 17–21 April 2018; pp. 415–418.
84. Rodríguez González, P.; Ling, G. Anodic behavior in $AlCl_3$-EMIC ionic liquid of Ti6Al4V alloy and its application for enhancing the adhesion strength of aluminum coatings. *Surf. Coat. Technol.* **2017**, *331*, 57–65. [CrossRef]
85. Yamagami, M.; Higashino, S.; Yamamoto, T.; Ikenoue, T.; Miyake, M.; Hirato, T. Aluminum Electrodeposition in Dry Air Atmosphere: Comparative Study of an Acetamide–AlCl3 Deep Eutectic Solvent and a 1-Ethyl-3-Methylimidazolium Chloride–$AlCl_3$ Ionic Liquid. *J. Electrochem. Soc.* **2022**, *169*, 062502. [CrossRef]
86. Elterman, V.A.; Shevelin, P.Y.; Yolshina, L.A.; Borozdin, A.V. Electrodeposition of aluminium from the chloroaluminate ionic liquid 1-ethyl-3-methylimidazolium chloride. *Electrochim. Acta* **2021**, *389*, 138715. [CrossRef]
87. Yang, Y.; Liu, S.; Chi, C.; Hao, J.; Zhao, J.; Xu, Y.; Li, Y. Electrodeposition of a continuous, dendrite-free aluminum film from an ionic liquid and its electrochemical properties. *J. Mater. Sci. Mater. Electron.* **2020**, *31*, 9937–9945. [CrossRef]
88. Jiang, Y.; Ding, J.; Luo, L.; Shi, P.; Wang, X. Electrodepositing aluminum coating on uranium from aluminum chloride-1-ethyl-3-methylimidazolium chloride ionic liquid. *Surf. Coat. Technol.* **2017**, *309*, 980–985. [CrossRef]
89. Wang, J.; Liu, X.; Xie, H.; Yin, H.; Song, Q.; Ning, Z. Effect of a Magnetic Field on the Electrode Process of Al Electrodeposition in a [Emim]Cl-$AlCl_3$ Ionic Liquid. *J. Phys. Chem. B* **2021**, *125*, 13744–13751. [CrossRef]
90. Takahashi, H.; Matsushima, H.; Ueda, M. Al Film Electrodeposition from the AlCl3-EMIC Electrolyte under a Magnetic Field. *J. Electrochem. Soc.* **2017**, *164*, H5165. [CrossRef]
91. Zhang, B.; Shi, Z.; Shen, L.; Liu, A.; Xu, J.; Hu, X. Electrodeposition of Al, Al-Li Alloy, and Li from an Al-Containing Solvate Ionic Liquid under Ambient Conditions. *J. Electrochem. Soc.* **2018**, *165*, D321. [CrossRef]
92. Yang, Y.; Hao, J.; Xue, J.; Liu, S.; Chi, C.; Zhao, J.; Xu, Y.; Li, Y. Co-electrodeposited Al-Ga composite electrode from ionic liquid with volume expansion adaptability in energy storage. *Mater. Lett.* **2021**, *303*, 130484. [CrossRef]
93. Yang, J.; Chang, L.; Jiang, L.; Wang, K.; Huang, L.; He, Z.; Shao, H.; Wang, J.; Cao, C.-N. Electrodeposition of Al-Mn-Zr ternary alloy films from the Lewis acidic aluminum chloride-1-ethyl-3-methylimidazolium chloride ionic liquid and their corrosion properties. *Surf. Coat. Technol.* **2017**, *321*, 45–51. [CrossRef]
94. Hibino, Y.; Azumi, K. Enhancement of Al-Ti Alloy Electrodeposition from $AlCl_3$-EMIC Ionic Liquid Based Bath by Mg Additive. *J. Electrochem. Soc.* **2019**, *166*, D776. [CrossRef]
95. Higashino, S.; Takeuchi, Y.; Miyake, M.; Ikenoue, T.; Tane, M.; Hirato, T. Tungsten(II) chloride hydrates with high solubility in chloroaluminate ionic liquids for the electrodeposition of Al–W alloy films. *J. Electroanal. Chem.* **2022**, *912*, 116238. [CrossRef]
96. Higashino, S.; Miyake, M.; Takahashi, A.; Matamura, Y.; Fujii, H.; Kasada, R.; Hirato, T. Evaluation of the hardness and Young's modulus of electrodeposited Al–W alloy films by nano-indentation. *Surf. Coat. Technol.* **2017**, *325*, 346–351. [CrossRef]
97. Höhlich, D.; Wachner, D.; Müller, M.; Scharf, I.; Lampke, T. Electrodeposition and characterisation of Al-W alloy films from ionic liquid. *IOP Conf. Ser. Mater. Sci. Eng.* **2018**, *373*, 012007. [CrossRef]
98. Peng, D.; Cong, D.; Song, K.; Ding, X.; Wang, X.; Bai, Y.; Yang, X.; Yin, C.; Zhang, Y.; Rao, J.; et al. Mirror-like Bright Al-Mn Coatings Electrodeposition from 1-Ethyl-3 Methylimidazolium Chloride-AlCl3-MnCl2 Ionic Liquids with Pyridine Derivatives. *Materials* **2021**, *14*, 6226. [CrossRef] [PubMed]
99. Chang, C.-C.; Sun, I.W. Template-Free Fabrication of Diameter-Modulated Co-Zn/Oxide Wires from a Chlorozincate Ionic Liquid by Using Pulse Potential Electrodeposition. *J. Electrochem. Soc.* **2017**, *164*, D425. [CrossRef]
100. He, W.; Shi, Z.; Liu, A.; Guan, J.; Yang, S. Electro-reduction of Cu_2O to Cu in urea/1-ethyl-3-methylimidazolium chloride. *J. Appl. Electrochem.* **2021**, *51*, 1145–1156. [CrossRef]
101. Lehmann, L.; Höhlich, D.; Mehner, T.; Lampke, T. Irregular Electrodeposition of Cu-Sn Alloy Coatings in [EMIM]Cl Outside the Glove Box with Large Layer Thickness. *Coatings* **2021**, *11*, 310. [CrossRef]
102. Bakkar, A.; Neubert, V. Electrodeposition of photovoltaic thin films from ionic liquids in ambient atmosphere: Gallium from a chloroaluminate ionic liquid. *J. Electroanal. Chem.* **2020**, *856*, 113656. [CrossRef]
103. Zhang, W.; Pesic, B. Electrochemical Behavior of PdCl2 in 1-Ethyl-3-Methylimidazolium Chloride Ionic Liquid at Pt-Ir Electrode. *J. Electrochem. Soc.* **2021**, *168*, 072506. [CrossRef]
104. Zhang, W.; Pesic, B. Electrochemistry of PdCl2 at glassy carbon electrode in 1-Ethyl-3-methylimidazolium chloride ionic liquid. *Electrochim. Acta* **2021**, *370*, 137818. [CrossRef]

105. Yang, Y.; Xu, C.; Hua, Y.; Wang, M.; Su, Z. Electrochemical preparation of Ni-La alloys from the EMIC-EG eutectic-based ionic liquid. *Ionics* **2017**, *23*, 1703–1710. [CrossRef]
106. Xu, X.; Sturm, S.; Zavasnik, J.; Rozman, K.Z. Electrodeposition of a Rare-Earth Iron Alloy from an Ionic-Liquid Electrolyte. *ChemElectroChem* **2019**, *6*, 2860–2869. [CrossRef]
107. Xi, X.; Song, S.; Nie, Z.; Ma, L. Electrodeposition and behavior of palladium in a room temperature ionic liquid. *Int. J. Electrochem. Sci.* **2017**, *12*, 1130–1145. [CrossRef]
108. Zhang, J.; Ma, X.; Zhang, J.; Yang, P.; An, M.; Li, Q. Electrodeposition of Cu-Zn alloy from EMImTfO ionic liquid/ethanol mixtures for replacing the cyanide zincate layer on Al alloy. *J. Alloy. Compd.* **2019**, *806*, 79–88. [CrossRef]
109. Pham, T.A.; Horwood, C.; Maiti, A.; Peters, V.; Bunn, T.; Stadermann, M. Solvation Properties of Silver and Copper Ions in a Room Temperature Ionic Liquid: A First-Principles Study. *J. Phys. Chem. B* **2018**, *122*, 12139–12146. [CrossRef]
110. Shao, M.; Li, S.; Jin, C.; Chen, M.; Huang, Z. Recovery of Pd(II) from Hydrochloric Acid Medium by Solvent Extraction–Direct Electrodeposition Using Hydrophilic/Hydrophobic ILs. *ACS Omega* **2020**, *5*, 27188–27196. [CrossRef]
111. Rani, M.A.A.; Hwang, J.; Matsumoto, K.; Hagiwara, R. Poly(vinyl chloride) Ionic Liquid Polymer Electrolyte Based on Bis(fluorosulfonyl)Amide for Sodium Secondary Batteries. *J. Electrochem. Soc.* **2017**, *164*, H5031. [CrossRef]
112. He, W.; Shi, Z.; Liu, F.; Yang, S. Electrodeposition of Copper Metal from the 1-Ethyl-3-methylimidazolium Fluoride ([EMIM]F)-urea-H_2O System Containing Cu_2O. *Electrochemistry* **2020**, *88*, 253–255. [CrossRef]
113. Sato, Y.; Maruyama, S.; Matsumoto, Y. Electrodeposition of metallic Cu from CuCl gas source transported into ionic liquid in a vacuum. *J. Vac. Sci. Technol. A* **2018**, *36*, 031516. [CrossRef]
114. Soulmi, N.; Porras-Gutierrez, A.-G.; Mordvinova, N.E.; Lebedev, O.I.; Rizzi, C.; Sirieix-Plénet, J.; Groult, H.; Dambournet, D.; Gaillon, L. Sn(TFSI)2 as a suitable salt for the electrodeposition of nanostructured Cu6Sn5–Sn composites obtained on a Cu electrode in an ionic liquid. *Inorg. Chem. Front.* **2019**, *6*, 248–256. [CrossRef]
115. Shimizu, M.; Sugiyama, Y.; Horita, M.; Yoshii, K.; Arai, S. Cation-Structure Effects on Zinc Electrodeposition and Crystallographic Orientation in Ionic Liquids. *ChemElectroChem* **2022**, *9*, e202200016. [CrossRef]
116. Chen, Y.-T.; Chen, P.-Y.; Ju, S.-P. Preparation of Ni nanotube-modified electrodes via galvanic displacement on sacrificial Zn templates: Solvent effects and attempts for non-enzymatic electrochemical detection of urea. *Microchem. J.* **2020**, *158*, 105172. [CrossRef]
117. Sousa, N.G.; Salgueira, J.F.S.; Sousa, C.P.; Campos, O.S.; Salazar-Banda, G.R.; Eguiluz, K.I.B.; de Lima-Neto, P.; Correia, A.N. Silver electrodeposition at room temperature protic ionic liquid 1-H-methylimidazolium hydrogen sulfate. *J. Mol. Liq.* **2020**, *313*, 113487. [CrossRef]
118. Kuang, Y.; Jiang, F.; Zhu, T.; Wu, H.; Yang, X.; Li, S.; Hu, C. One-step electrodeposition of superhydrophobic copper coating from ionic liquid. *Mater. Lett.* **2021**, *303*, 130579. [CrossRef]
119. Li, M.; Li, Y. Electrodeposition of Zinc from Zinc Oxide and Zinc Chloride in 1-Methylimidazolium Trifluoromethylsulfonate Ionic Liquid. *Prot. Met. Phys. Chem. Surf.* **2020**, *56*, 180–188. [CrossRef]
120. Motobayashi, K.; Shibamura, Y.; Ikeda, K. Origin of a High Overpotential of Co Electrodeposition in a Room-Temperature Ionic Liquid. *J. Phys. Chem. Lett.* **2020**, *11*, 8697–8702. [CrossRef] [PubMed]
121. Chen, M.; Li, S.; Jin, C.; Shao, M.; Huang, Z. Selective recovery of platinum by combining a novel reusable ionic liquid with electrodeposition. *Sep. Purif. Technol.* **2021**, *259*, 118204. [CrossRef]
122. Wang, N.; Wang, Q.; Lu, W.; Ru, M.; Yang, Y. Extraction and stripping of platinum (IV) from acidic chloride media using guanidinium ionic liquid. *J. Mol. Liq.* **2019**, *293*, 111040. [CrossRef]
123. Guinea, E.; Salicio-Paz, A.; Iriarte, A.; Grande, H.-J.; Medina, E.; García-Lecina, E. Robust Aluminum Electrodeposition from Ionic Liquid Electrolytes Containing Light Aromatic Naphta as Additive. *ChemistryOpen* **2019**, *8*, 1094–1099. [CrossRef]
124. Chen, J.-A.; Chen, P.-Y.; Sun, I.W. An Assessment of Aluminum Electrodeposition from Aluminum Chloride/4-ethylpyridine Ionic Liquid at Ambient Temperature. *J. Electrochem. Soc.* **2022**, *169*, 052505. [CrossRef]
125. Suneesh, P.V.; Ramachandran, T.; Satheesh Babu, T.G. Electrodeposition of Al-Zr-Cu Ternary Alloy from AlCl3-Et3NHCl Ionic Liquid containing Acetylacetonates of Copper and Zirconium. *Mater. Today Proc.* **2018**, *5*, 16640–16645. [CrossRef]
126. Fong, J.-D.; Chen, P.-Y.; Sun, I.W. Template-Free Electrodeposition of Net-Like Co-Al/Oxide Structures from a Lewis Acidic Chloroaluminate Room Temperature Ionic Liquid Using a Potential Step Method. *J. Electrochem. Soc.* **2018**, *165*, D716. [CrossRef]
127. Shao, Y.-A.; Chen, Y.-T.; Chen, P.-Y. Cu and CuPb electrodes prepared via potentiostatic electrodeposition from metal oxides in hydrophobic protic amide-type ionic liquid/water mixture under ambient air for nonenzymatic nitrate reduction. *Electrochim. Acta* **2019**, *313*, 488–496. [CrossRef]
128. Shao, Y.-A.; Chen, Y.-T.; Chen, P.-Y. Cu and CuPb Electrodes Electrodeposited from Metal Oxides in Hydrophobic Protic Amide-Type Ionic Liquid/Water Mixture for Nonenzymatic Glucose Oxidation. *J. Electrochem. Soc.* **2019**, *166*, D221. [CrossRef]
129. Chen, P.; Richter, J.; Wang, G.; Li, D.; Pietsch, T.; Ruck, M. Ionometallurgical Step-Electrodeposition of Zinc and Lead and its Application in a Cycling-Stable High-Voltage Zinc-Graphite Battery. *Small* **2021**, *17*, 2102058. [CrossRef]
130. Yeh, H.-W.; Tang, Y.-H.; Chen, P.-Y. Electrochemical study and extraction of Pb metal from Pb oxides and Pb sulfate using hydrophobic Brønsted acidic amide-type ionic liquid: A feasibility demonstration. *J. Electroanal. Chem.* **2018**, *811*, 68–77. [CrossRef]

131. Kono, S.; Takao, K.; Arai, T. Direct and Selective Electrodeposition of Palladium from Betainium Bis(trifluoromethanesulfonyl)imide Ionic Liquid Phase after Solvent Extraction together with Other Platinum Group Metals. *Trans. At. Energy Soc. Jpn.* **2020**, *19*, 76–84. [CrossRef]
132. Wang, Z.; Wu, T.; Geng, X.; Ru, J.; Hua, Y.; Bu, J.; Xue, Y.; Wang, D. The role of electrolyte ratio in electrodeposition of nanoscale FeCr alloy from choline chloride-ethylene glycol ionic liquid: A suitable layer for corrosion resistance. *J. Mol. Liq.* **2022**, *346*, 117059. [CrossRef]
133. Danilov, F.I.; Bogdanov, D.A.; Smyrnova, O.V.; Korniy, S.A.; Protsenko, V.S. Electrodeposition of Ni–Fe alloy from a choline chloride-containing ionic liquid. *J. Solid State Electrochem.* **2022**, *26*, 939–957. [CrossRef]
134. Rosoiu, S.P.; Pantazi, A.G.; Petica, A.; Cojocaru, A.; Costovici, S.; Zanella, C.; Visan, T.; Anicai, L.; Enachescu, M. Comparative Study of Ni-Sn Alloys Electrodeposited from Choline Chloride-Based Ionic Liquids in Direct and Pulsed Current. *Coatings* **2019**, *9*, 801. [CrossRef]
135. Protsenko, V.S.; Bogdanov, D.A.; Korniy, S.A.; Kityk, A.A.; Baskevich, A.S.; Danilov, F.I. Application of a deep eutectic solvent to prepare nanocrystalline Ni and Ni/TiO_2 coatings as electrocatalysts for the hydrogen evolution reaction. *Int. J. Hydrog. Energy* **2019**, *44*, 24604–24616. [CrossRef]
136. Alesary, H.F.; Khudhair, A.F.; Rfaish, S.Y.; Ismail, H.K. Effect of Sodium Bromide on the Electrodeposition of Sn, Cu, Ag and Ni from a Deep Eutectic Solvent-Based Ionic Liquid. *Int. J. Electrochem. Sci.* **2019**, *14*, 7116–7132. [CrossRef]
137. Fashu, S.; Mudzingwa, L.; Khan, R.; Tozvireva, M. Electrodeposition of high corrosion resistant Ni–Sn–P alloy coatings from an ionic liquid based on choline chloride. *Trans. IMF* **2018**, *96*, 20–26. [CrossRef]
138. Panzeri, G.; Pedrazzetti, L.; Rinaldi, C.; Nobili, L.; Magagnin, L. Electrodeposition of Nanostructured Cobalt Films from Choline Chloride-Ethylene Glycol Deep Eutectic Solvent. *J. Electrochem. Soc.* **2018**, *165*, D580. [CrossRef]
139. Pereira, N.M.; Brincoveanu, O.; Pantazi, A.G.; Pereira, C.M.; Araújo, J.P.; Fernando Silva, A.; Enachescu, M.; Anicai, L. Electrodeposition of Co and Co composites with carbon nanotubes using choline chloride-based ionic liquids. *Surf. Coat. Technol.* **2017**, *324*, 451–462. [CrossRef]
140. Alesary, H.F.; Ismail, H.K.; Hameid Odda, A.; Watkins, M.J.; Arkan Majhool, A.; Ballantyne, A.D.; Ryder, K.S. Influence of different concentrations of nicotinic acid on the electrochemical fabrication of copper film from an ionic liquid based on the complexation of choline chloride-ethylene glycol. *J. Electroanal. Chem.* **2021**, *897*, 115581. [CrossRef]
141. Yavuz, A.; Yilmaz Erdogan, P.; Zengin, H.; Zengin, G. Electrodeposition and Characterisation of Zn-Co Alloys from Ionic Liquids on Copper. *J. Electron. Mater.* **2022**, *51*, 5253–5261. [CrossRef]
142. Marín-Sánchez, M.; Gracia-Escosa, E.; Conde, A.; Palacio, C.; García, I. Deposition of Zinc–Cerium Coatings from Deep Eutectic Ionic Liquids. *Materials* **2018**, *11*, 2035. [CrossRef]
143. Fashu, S.; Khan, R.; Zulfiqar, S. Ternary Zn–Mn–Sn alloy electrodeposition from an ionic liquid based on choline chloride. *Trans. IMF* **2017**, *95*, 217–225. [CrossRef]
144. Popescu, A.M.; Soare, V.; Demidenko, O.; Moreno, J.M.C.; Neacsu, E.I.; Donath, C.; Constantin, V. Recovery of Silver and Gold from Electronic Waste by Electrodeposition in Ethaline Ionic Liquid. *Rev. Chim.* **2020**, *71*, 122–132. [CrossRef]
145. Du, C.; Yang, H.; Chen, X.-B.; Wang, L.; Dong, H.; Ning, Y.; Lai, Y.; Jia, J.; Zhao, B. Effect of coordinated water of hexahydrate on nickel platings from choline–urea ionic liquid. *J. Mater. Sci.* **2018**, *53*, 10758–10771. [CrossRef]
146. Li, M.; Chen, B.Q.; Xiong, T.T.; Gao, L.X.; Du, C.; Zhu, Y.N.; Zhang, S.M. Electrodeposition of Pr-Mg-Co ternary alloy films from the choline chloride-Urea ionic liquids and their corrosion properties. *J. Dispers. Sci. Technol.* **2020**, *41*, 941–947. [CrossRef]
147. Li, M.; Chen, B.Q.; He, M.; Xiong, T.; Gao, L. Electrodeposition of Pr-Mg-Ni ternary alloy films from the choline chloride-urea ionic liquid and their corrosion properties. *Anti-Corros. Methods Mater.* **2018**, *65*, 437–443. [CrossRef]
148. Shi, T.; Zou, X.; Wang, S.; Pang, Z.; Tang, W.; Li, G.; Xu, Q.; Lu, X. Electrodeposition of Sn-Co-Ni and Sn-Co-Zn Alloy Coatings on Copper Substrate in a Deep Eutectic Solvent and Their Characterization. *Int. J. Electrochem. Sci.* **2020**, *15*, 7493–7507. [CrossRef]
149. Golgovici, F.; Ionascu, F.G.; Prodana, M.; Demetrescu, I. Simultaneously Embedding Indomethacin and Electrodeposition of Polypyrrole on Various CoCr Alloys from Ionic Liquids. *Materials* **2022**, *15*, 4714. [CrossRef]
150. Zhang, B.; Yao, Y.; Shi, Z.; Xu, J.; Wang, Z. Direct Electrochemical Deposition of Lithium from Lithium Oxide in a Highly Stable Aluminium-Containing Solvate Ionic Liquid. *ChemElectroChem* **2018**, *5*, 3368–3372. [CrossRef]
151. Tachikawa, N.; Kasai, R.; Yoshii, K.; Watanabe, M.; Katayama, Y. Electrochemical Deposition and Dissolution of Lithium on a Carbon Fiber Composite Electrode in a Solvate Ionic Liquid. *Electrochemistry* **2017**, *85*, 667–670. [CrossRef]
152. Berger, C.A.; Ceblin, M.U.; Jacob, T. Lithium Deposition from a Piperidinium–based Ionic Liquid: Rapping Dendrites on the Knuckles. *ChemElectroChem* **2017**, *4*, 261–265. [CrossRef]
153. He, J.-W.; Gu, Y.; Wang, W.-W.; Wang, J.-H.; Chen, Z.-B.; He, H.-Y.; Wu, Q.-H.; Yan, J.-W.; Mao, B.-W. Structures of Solid-Electrolyte Interphases and Impacts on Initial-Stage Lithium Deposition in Pyrrolidinium-Based Ionic Liquids. *ChemElectroChem* **2021**, *8*, 62–69. [CrossRef]
154. Galindo, M.; Sebastián, P.; Cojocaru, P.; Gómez, E. Electrodeposition of aluminium from hydrophobic perfluoro-3-oxa-4,5 dichloro-pentan-sulphonate based ionic liquids. *J. Electroanal. Chem.* **2018**, *820*, 41–50. [CrossRef]
155. Oriani, A.V.; Cojocaru, P.; Monzani, C.; Vallés, E.; Gómez, E. Aluminium electrodeposition from a novel hydrophobic ionic liquid tetramethyl guanidinium-perfluoro-3-oxa-4,5 dichloro-pentan-sulphonate. *J. Electroanal. Chem.* **2017**, *793*, 85–92. [CrossRef]
156. Yu, X.; Cui, J.; Liu, C.; Yuan, F.; Guo, Y.; Deng, T. Separation of magnesium from high Mg/Li ratio brine by extraction with an organic system containing ionic liquid. *Chem. Eng. Sci.* **2021**, *229*, 116019. [CrossRef]

157. Rajagopal, V.; Velayutham, D.; Suryanarayanan, V.; Kathiresan, M.; Ho, K.C. Electrochemical fabrication of dendritic silver–copper bimetallic nanomaterials in protic ionic liquid for electrocarboxylation. *J. Taiwan Inst. Chem. Eng.* **2018**, *87*, 158–164. [CrossRef]
158. Song, Y.; Tsuchida, Y.; Matsumiya, M.; Tsunashima, K. Recovery of ruthenium by solvent extraction and direct electrodeposition using ionic liquid solution. *Hydrometallurgy* **2018**, *181*, 164–168. [CrossRef]
159. Matsumiya, M.; Song, Y.; Tsuchida, Y.; Ota, H.; Tsunashima, K. Recovery of platinum by solvent extraction and direct electrodeposition using ionic liquid. *Sep. Purif. Technol.* **2019**, *214*, 162–167. [CrossRef]
160. García-Montoya, M.F.; Gutiérrez-Granados, S.; Méndez-Quezada, J.Y.; Cholico-González, D.F.; Ponce de León, C.; Hernández-Perales, L.; Ávila-Rodríguez, M. Electrochemistry of Rhodium (III) in Trihexil(tetradecyl) Phosphonium Bis(2,4,4-trimethylpentyl) Phosphinate Ionic Liquid (Cyphos IL 104 ®) and Its Deposition. *ECS Trans.* **2018**, *84*, 1. [CrossRef]
161. Sanchez-Cupido, L.; Pringle, J.M.; Siriwardana, A.L.; Unzurrunzaga, A.; Hilder, M.; Forsyth, M.; Pozo-Gonzalo, C. Water-Facilitated Electrodeposition of Neodymium in a Phosphonium-Based Ionic Liquid. *J. Phys. Chem. Lett.* **2019**, *10*, 289–294. [CrossRef]
162. Deferm, C.; Malaquias, J.C.; Onghena, B.; Banerjee, D.; Luyten, J.; Oosterhof, H.; Fransaer, J.; Binnemans, K. Electrodeposition of indium from the ionic liquid trihexyl(tetradecyl)phosphonium chloride. *Green Chem.* **2019**, *21*, 1517–1530. [CrossRef]
163. Bourbos, E.; Giannopoulou, I.; Karantonis, A.; Paspaliaris, I.; Panias, D. Reduction of Light Rare Earths and a Proposed Process for Nd Electrorecovery Based on Ionic Liquids. *J. Sustain. Metall.* **2018**, *4*, 395–406. [CrossRef]
164. Gao, M.Y.; Yang, C.; Zhang, Q.B.; Zeng, J.R.; Li, X.T.; Hua, Y.X.; Xu, C.Y.; Li, Y. Electrochemical Preparation of Ni-La Alloy Films from N-butyl-N-Methyl Pyrrolidinium Dicyanamide Ionic Liquid as Electrocatalysts for Hydrogen Evolution Reaction. *J. Electrochem. Soc.* **2017**, *164*, D778. [CrossRef]
165. Periyapperuma, K.; Pringle, J.M.; Sanchez-Cupido, L.; Forsyth, M.; Pozo-Gonzalo, C. Fluorine-free ionic liquid electrolytes for sustainable neodymium recovery using an electrochemical approach. *Green Chem.* **2021**, *23*, 3410–3419. [CrossRef]
166. Sano, H.; Kitta, M.; Shikano, M.; Matsumoto, H. Effect of Temperature on Li Electrodeposition Behavior in Room-Temperature Ionic Liquids Comprising Quaternary Ammonium Cation. *J. Electrochem. Soc.* **2019**, *166*, A2973. [CrossRef]
167. Schuett, F.M.; Heubach, M.-K.; Mayer, J.; Ceblin, M.U.; Kibler, L.A.; Jacob, T. Electrodeposition of Zinc onto Au(111) and Au(100) from the Ionic Liquid [MPPip][TFSI]. *Angew. Chem. Int. Ed.* **2021**, *60*, 20461–20468. [CrossRef] [PubMed]
168. Nishi, N.; Ezawa, K.; Sakka, T. In Situ Surface Roughness Analysis of Electrodeposited Co Films in an Ionic Liquid Using Electrochemical Surface Plasmon Resonance: Effect of Leveling Additives. *J. Electrochem. Soc.* **2021**, *168*, 072505. [CrossRef]
169. Wang, Y.-S.; Chen, P.-Y. Electrochemical Study and Electrodeposition of Zn-Ni Alloys in an Imide-Type Hydrophobic Room-Temperature Ionic Liquid: Feasibility of Using Metal Chlorides as the Metal Sources. *J. Electrochem. Soc.* **2018**, *165*, D76. [CrossRef]
170. Yavuz, A.; Yilmaz, N.F.; Artan, M. Fe-Cu Alloy-Based Flexible Electrodes from Ethaline Ionic Liquid. *J. Electron. Mater.* **2021**, *50*, 3478–3487. [CrossRef]
171. Li, M.; Li, Y. Aluminum Electrodeposition using AlCl3/urea Ionic Liquid. *Int. J. Electrochem. Sci.* **2020**, *15*, 8498–8505. [CrossRef]
172. Lambri, O.A.; Weidenfeller, B.; Bonifacich, F.G.; Mohr-Weidenfeller, L.; Lambri, F.D.; Xu, J.; Zelada, G.I.; Endres, F. Study of the damping behaviour in samples consisting of iron electro-deposited on copper in an ionic liquid. *J. Alloy. Compd.* **2022**, *918*, 165462. [CrossRef]
173. Protsenko, V.S.; Butyrina, T.E.; Bobrova, L.S.; Korniy, S.A.; Danilov, F.I. Electrochemical Corrosion Behavior of Ni–TiO_2 Composite Coatings Electrodeposited from a Deep Eutectic Solvent-Based Electrolyte. *Coatings* **2022**, *12*, 800.
174. Ramírez, C.; Bozzini, B.; Calderón, J.A. Electrodeposition of copper from triethanolamine as a complexing agent in alkaline solution. *Electrochim. Acta* **2022**, *425*, 140654. [CrossRef]
175. Bhujbal, A.V.; Rout, A.; Venkatesan, K.A.; Bhanage, B.M. Electrochemical Fabrication of Copper and Tin Micro-Crystals from a Protic Ionic Liquid Medium. *ChemistrySelect* **2020**, *5*, 3694–3699. [CrossRef]
176. Maniam, K.K.; Paul, S. Progress in Electrodeposition of Zinc and Zinc Nickel Alloys Using Ionic Liquids. *Appl. Sci.* **2020**, *10*, 5321. [CrossRef]
177. Lahiri, A.; Endres, F. Review—Electrodeposition of Nanostructured Materials from Aqueous, Organic and Ionic Liquid Electrolytes for Li-Ion and Na-Ion Batteries: A Comparative Review. *J. Electrochem. Soc.* **2017**, *164*, D597. [CrossRef]
178. Mittal, N.; Tien, S.; Lizundia, E.; Niederberger, M. Hierarchical Nanocellulose-Based Gel Polymer Electrolytes for Stable Na Electrodeposition in Sodium Ion Batteries. *Small* **2022**, *18*, 2107183. [CrossRef]
179. Miki, A.; Nishikawa, K.; Kamesui, G.; Matsushima, H.; Ueda, M.; Rosso, M. In situ interferometry study of ionic mass transfer phenomenon during the electrodeposition and dissolution of Li metal in solvate ionic liquids. *J. Mater. Chem. A* **2021**, *9*, 14700–14709. [CrossRef]
180. Zhang, S.; Yamazawa, T.; Sakka, T.; Nishi, N. In Situ Electrochemical Surface Plasmon Resonance Study on Lithium Underpotential Deposition and Stripping in Bis(fluorosulfonyl)amide-Based Ionic Liquids. *J. Phys. Chem. C* **2022**, *126*, 9551–9558. [CrossRef]
181. Khosravi, R.; Azizi, A.; Ghaedrahmati, R.; Gupta, V.K.; Agarwal, S. Adsorption of gold from cyanide leaching solution onto activated carbon originating from coconut shell—Optimization, kinetics and equilibrium studies. *J. Ind. Eng. Chem.* **2017**, *54*, 464–471. [CrossRef]
182. Meng, Q.; Yan, X.; Li, G. Eco-friendly and reagent recyclable gold extraction by iodination leaching-electrodeposition recovery. *J. Clean. Prod.* **2021**, *323*, 129115. [CrossRef]
183. Zhang, Y.; Nishi, N.; Sakka, T. One-step fabrication of Au@Pd core-shell bimetallic nanofibers at the interface between water and redox-active ionic liquid. *Electrochim. Acta* **2019**, *325*, 134919. [CrossRef]

184. Sobek, D.; Bhattacharyya, S. Dispensing of Alkali Metals via Electrodeposition Using Alkali Metal Salts in Ionic Liquids. US20200109481A1, 9 April 2020.
185. Jiang, F.; Shi, W.; Wu, H.; Zhao, X.; Li, Y.; Li, S. A kind of Method of Simple System Electrodepositing Zinc Coating. CN108754556A, 6 November 2018.
186. Zhou, G.; Wang, W.; Zhang, R.; Wang, S.; Wu, M.; Nível, Q.; Mitsuzaki, S.; Chen, Z. Method for Preparing Super-Hydrophobic Zn-Fe Alloy Coating in Eutectic Ionic Liquid through Electrodeposition. CN113174617A, 27 July 2021.
187. Fan, J.; Li, J.; Yang, X.; Chen, Y.; Shi, W.; Liu, H. The Method that High Current Density Electrochemistry Prepares Spelter Coating in Ionic Liquid. CN108754557A, 6 November 2018.
188. Xue, X.; Wang, Y.; Yue, H.; Zhou, S. The Method that the Hydrated Chromium Trichloride Ionic Liquid Electrodeposition of Choline Chloride Six Prepares Crome Metal. CN107254698A, 17 October 2017.
189. Zhang, Q.; Yang, C.; Hua, Y.; Xu, C.; Li, Y. The Method that Electro-Deposition Prepares Self-Cradling Type Nanometer Cobalt Bimetallic Phosphide Catalytic Hydrogen Evolution Electrode Material in Eutectic Type Ionic Liquid. CN108360030A, 23 January 2018.
190. Zhang, Q.; Gao, M.; Yang, C.; Hua, Y.; Xu, C.; Li, J.; Li, Y. Method for Preparing High-Catalytic Oxygen Evolution Performance Nano Porous Nickel-Iron-Sulfur Alloy by Electrodeposition in Eutectic Ionic Liquid. CN107335450B, 7 February 2020.
191. Um, M.; Song, Y.; Yang, P.; Zhang, J.; Feng, Z. Ionic Liquid Gold Plating Solution Containing Coordination Agent and Additive and Gold Plating Method Adopting Ionic Liquid Gold Plating Solution. CN106676595A, 17 May 2017.
192. Li, Y.; Li, M. A Method of Preparing Metallic Zinc Using Ionic Liquid Electrolytic Oxidation Zinc. CN108315763A, 24 July 2018.
193. Shi, Z.; Liu, A.; Wang, Z.; Gao, B.; Hu, X.; Liu, F.; Tao, W.; Yang, Y.; Yu, J. A Kind of Method that Electrodeposition Process Prepares Metallic Lead. CN109536994A, 29 March 2019.